

The systematics of the Mongolepidida (Chondrichthyes) and the Ordovician origins of the clade

Plamen Andreev, Michael I Coates, Valentina Karatajūtė-Talimaa, Richard M Shelton, Paul R Cooper, Nian-Zhong Wang, Ivan J Sansom

The Mongolepidida is an Order of putative basal chondrichthyan fish, originally erected to unite taxa from the Lower Silurian of Mongolia. The present study reassesses mongolepid systematics through the examination of the developmental, histological and morphological characteristics of scale-based specimens from the Upper Ordovician Harding Sandstone (Colorado, USA) and the Upper Llandovery–Lower Wenlock Yimugantawu (Tarim Basin, China), Xiushan (Guizhou Province, China) and Chagat (north-western Mongolia) Formations.

The inclusion of the Mongolepidida within the Class Chondrichthyes is supported on the basis of a suite of scale attributes (areal odontode deposition, linear odontocomplex structure and lack of enamel, cancellous bone and hard-tissue resorption) shared with crown chondrichthyans (e.g. ctenacanthiforms). The mongolepid dermal skeleton exhibits a rare type of atubular dentine (lamellin) that is regarded as one of the diagnostic features of the Order within crown gnathostomes.

The previously erected Mongolepididae and Shiqianolepidae Families are revised, differentiated by scale-base histology and expanded to include the genera *Rongolepis* and *Xinjiangichthys*, respectively. A newly described mongolepid species (*Solinalepis levis* gen. et sp. nov.) from the Ordovician of North America is treated as Family incertae sedis, as it possesses a type of basal bone tissue (acellular and vascular) that has yet to be documented in other mongolepids.

This study extends the stratigraphic and palaeogeographic range of Mongolepidida and adds further evidence for an early diversification of the Chondrichthyes in the Ordovician Period, 50 million years prior to the first recorded appearance of chondrichthyan teeth in the Lower Devonian.

The systematics of the Mongolepidida (Chondrichthyes) and the Ordovician origins of the clade

Plamen S. Andreev¹, Michael I. Coates², Valentina Karatajūtė-Talimaa³, Richard M. Shelton⁴, Paul R. Cooper⁴, Nian-Zhong Wang^{5†} and Ivan J. Sansom¹

¹School of Geography, Earth and Environmental Sciences, University of Birmingham, Edgbaston, Birmingham B15 2TT, UK

²Department of Organismal Biology and Anatomy, University of Chicago, Chicago, Illinois 60637-1508, USA

³Department of Geology and Mineralogy, Vilnius University, M.K. Ciurlionio 21/27, LT-03101 Vilnius, Lithuania

⁴School of Dentistry, College of Medical and Dental Sciences, University of Birmingham, St Chad's Queensway, Birmingham B4 6NN, UK

⁵Laboratory of Evolutionary Systematics of Vertebrates, Institute of Vertebrate Palaeontology and Palaeoanthropology, Chinese Academy of Sciences, PO Box 643, Beijing 100044, China; deceased

Corresponding authors

Plamen Andreev, p.andreev@bham.ac.uk

Ivan Sansom, i.j.sansom@bham.ac.uk

Abstract

The Mongolepidida is an Order of putative basal chondrichthyan fish, originally erected to unite taxa from the Lower Silurian of Mongolia. The present study reassesses mongolepid systematics through the examination of the developmental, histological and morphological characteristics of scale-based specimens from the Upper Ordovician Harding Sandstone (Colorado, USA) and the Upper Llandovery–Lower Wenlock Yimugantawu (Tarim Basin, China), Xiushan (Guizhou Province, China) and Chargat (north-western Mongolia) Formations.



The inclusion of the Mongolepidida within the Class Chondrichthyes is supported on the basis of a suite of scale attributes (areal odontode deposition, linear odontocomplex structure and lack of enamel, cancellous bone and hard-tissue resorption) shared with crown chondrichthyans (e.g. ctenacanthiforms). The mongolepid dermal skeleton exhibits a rare type of atubular dentine (lamellin) that is regarded as one of the diagnostic features of the Order within crown gnathostomes.

The previously erected Mongolepididae and Shiqianolepididae Families are revised, differentiated by scale-base histology and expanded to include the genera *Rongolepis* and *Xinjiangichthys*, respectively. A newly described mongolepid species (*Solinalepis levis* gen. et sp. nov.) from the Ordovician of North America is treated as Family incertae sedis, as it possesses a type of basal bone tissue (acellular and vascular) that has yet to be documented in other mongolepids.

This study extends the stratigraphic and palaeogeographic range of Mongolepidida and adds further evidence for an early diversification of the Chondrichthyes in the Ordovician Period, 50 million years prior to the first recorded appearance of chondrichthyan teeth in the Lower Devonian.

Keywords Mongolepids, *Solinalepis* gen. nov., Ordovician, Scales, Morphogenesis, Odontocomplex

INTRODUCTION

Middle Ordovician to Upper Silurian strata have yielded a number of isolated scale remains that have been assigned to the chondrichthyans with varying degrees of confidence; a 50 million year record pre-dating the first appearance in the Devonian of clearly identifiable chondrichthyan teeth (*Leonodus* and *Celtiberina* Botella et al., 2009) and the earliest articulated specimens (*Doliodus* Miller, Cloutier & Turner, 2003; Maisey, Miller & Turner, 2009 and *Antarctilamna* Young, 1982). These, largely microscopic, remains include the elegeptolepids (Karatajūtė-Talimaa, 1973  Andreev et al., submitted  nacanthids (Zhu, 1998; Sansom, Wang & Smith, 2005), taxa such as *Tezakia* and *Canyonlepis* from the Ordovician of North America (Sansom, Smith & Smith, 1996; Andreev et al., 2015), *Tantalepis* (Sansom et al., 2012), *Kannathalepis* (Märss & Gagnier, 2001) and *Pilolepis* (Thorsteinsson, 1973), and, perhaps the most widely distributed and diverse collection of what Ørvig and Bendix-Almgreen, quoted in Karatajūtė-Talimaa (1995), referred to as ‘praechondrichthyes’, the mongolepids (Karatajūtė-Talimaa et al., 1990; Karatajūtė-Talimaa & Predtecheskyj, 1995; Sansom, Aldridge & Smith, 2000). It is the latter which this work concentrates on, re-assessing and re-defining previously described members of the Mongolepidida, and describing a new taxon that extends the range of the Order into the Ordovician, adding further evidence for a diversification of early chondrichthyans as part of the Great

Ordovician Biodiversification Event that encompasses a wide variety of taxa, both invertebrate (e.g. Webby, Paris & Droser, 2004; Servais et al., 2010) and vertebrate (Sansom, Smith & Smith, 2001; Turner, Blieck & Nowlan, 2004).

Previous work on mongolepids

Mongolepids were first described by Karatajūtė-Talimaa et al. (1997) from the Chargat Formation (Upper Llandovery–Lower Wenlock) in north-western Mongolia, together with a diverse assemblage of early vertebrates including pteraspitomorphs (Karatajūtė-Talimaa, unpublished data), thelodonts (Žigaitė, Karatajūtė-Talimaa & Blieck, 2011), acanthodian and elegeptolepids. The first erected species, *Mongolepis rozmanaе*, was subsequently added to with the description of *Teslepis jucunda* Karatajūtė-Talimaa & Novitskaya (1992) and *Sodolepis lucens* Karatajūtė-Talimaa & Novitskaya (1997), also from the Chargat Formation. Recently the stratigraphic ranges of *Mongolepis* and *Teslepis* have been extended to include Aeronian (Middle Llandovery) and Sheinwoodian (Lower Wenlock) sedimentary sequences from Altai and Tuva (Sennikov et al., 2015). *Shiqianolepis hollandi* from the Xiushan Formation (Telychian) of south China was also placed within the Order by Sansom, Aldridge & Smith (2000), although a new Family, the Shiqianolepidae, was erected based upon an interpretation of the scale growth patterns within mongolepids. Additional material from the upper Llandovery of the Tarim Basin (Xinjiang Uygyr Autonomous Region, north-west China) is also referable to the group (unpublished data). Thus, to date, the distribution of mongolepids has been limited to a very narrow time frame (Llandovery–Wenlock) and is concentrated within the Mongol-Tuva, Altai, South China and Tarim tectonic blocks. The taxonomic placement of the group has been greatly hampered by

the absence of articulated specimens that exhibit any anatomical detail of the mongolepid bodyplan (Karatajūtė-Talimaa et al., 1990; Karatajūtė-Talimaa, 1995)

MATERIAL AND METHODS

All examined material consists of isolated scales extracted by petroleum ether or acetic acid disaggregation of rock samples from the Sandbian Harding Sandstone of central Colorado, USA, the Upper Llandovery–Lower Wenlock Chagat Formation of north-western Mongolia, the lower and upper members of the Telychian Yimugantawu Formation of Xinjiang (Tarim Basin, China) and the lower Member of the Telychian Xiushan Formation (Guizhou Province, China).

Scale morphology was documented using the JEOL JSM-6060 and Zeiss EVO LS scanning electron microscopes at the School of Dentistry of the University of Birmingham, UK. Prior to imaging specimens were sputter-coated with a 25 nm-thick layer of gold/palladium alloy.

For the purpose of studying scale histology and internal structure, doubly polished thin sections of scales were examined with Nomarski differential interference contrast microscopy (using a ‘Zeiss Axioskop Pol’ polarization microscope) and scanning electron microscopy (using a JEOL JSM-6060 SEM at the School of Dentistry, University of Birmingham, UK).

Scale examination with X-ray radiation was performed with the SkyScan 1172 microtomography scanner at the School of Dentistry, University of Birmingham, UK.

The acquired microradiographs (tomographic projections) were taken at 0.3° intervals over a 180° rotation cycle at exposure times of 400 ms, using a 0.5 mm thick X-ray attenuating Al filter. These image data were processed with the SkyScan NRecon reconstruction software for the purpose of generating sets of microtomograms that were converted into volume renderings in Amira 5.4 3D analysis software.

Figured specimens are housed in the Lapworth Museum of Geology, University of Birmingham, UK (BU prefix), the Nanjing Institute of Geology and Palaeontology, Chinese Academy of Sciences, Nanjing, China (NIGP prefix) and the Institute of Vertebrate Paleontology and Paleoanthropology, Chinese Academy of Sciences, Beijing, China (IVPP V prefix).

Definitions of terms

The interpretations of the terms (Fig. 1) employed in the descriptions of fossil scales follow Andreev et al. (2015). The rationale behind this is to improve identification of homologous scale structures across taxa by introducing a standardized terminology.

SYSTEMATIC PALAEONTOLOGY

Class CHONDRICHTHYES Huxley, 1880

Order MONGOLEPIDIDA Karatajūtė-Talimaa, Novitskaya, Rozman & Sodov, 1990

Included Families

Mongolepididae Karatajūtė-Talimaa et al., 1990

Shiqianolepidae Sansom, Aldridge & Smith, 2000

Emended diagnosis

Chondrichthyans with polyodontode growing scale crowns formed by multiple antero-posteriorly oriented primary odontocomplex rows. Odontode size within each row increases gradually towards the posterior of the scale. Individual odontodes formed exclusively of isotropically and spherically mineralised atubular, acellular dentine (lamellin).

Remarks

The current study has determined scale crown growth (*sensu* Reif, 1978) to be a characteristic shared by all mongolepid taxa (see Discussion for details), contrary to previous interpretations of synchronomorial development of scale odontodes in Mongolian mongolepid species (Karatajūtė-Talimaa et al., 1990; Karatajūtė-Talimaa & Novitskaya, 1992, 1997). Under the revised definition of the Order, the Mongolepidida retains the Families Mongolepididae (Karatajūtė-Talimaa et al., 1990) and Shiqianolepidae (Sansom, Aldridge & Smith, 2000), yet *contra* Sansom, Aldridge & Smith (2000) these are newly differentiated on the basis of base histology (see below) and are expanded to also include the genera *Rongolepis* Sansom, Aldridge & Smith, 2000 and *Xinjiangichthys* Wang et al., 1998, respectively. *Solinalepis levis* gen. et sp.

nov. is also added to the Order, but placed within incertae sedis at Family-grade due to the absence of clearly defined characters at this taxonomic level.

Family MONGOLEPIDIDAE Karatajūtė-Talimaa, Novitskaya, Rozman & Sodov, 1990

Included Genera

Mongolepis Karatajūtė-Talimaa et al., 1990

Teslepis Karatajūtė-Talimaa & Novitskaya, 1992

Sodolepis Talimaa & Novitskaya, 1997

Rongolepis Sansom, Aldridge & Smith, 2000

Emended diagnosis

Mongolepids possessing scale bases composed of acellular bone tissue with plywood-like layering.

Remarks

Scale-derived phylogenetic data (Andreev et al., unpublished data) identify two monophyletic groups inside Mongolepidida distinguished by differences in the bone histology of the scale base. These substitute the scale-crown developmental characteristics that have been used previously by Sansom, Aldridge & Smith (2000) to establish the Family structure of the Mongolepidida.

183

184 Genus **MONGOLEPIS** Karatajūtė-Talimaa, Novitskaya, Rozman & Sodov, 1990

185 **Type and only species**

186 *Mongolepis rozmanae* Karatajūtė-Talimaa *et al.* 1990, from the Chargat Formation,
 187 Salhit regional Stage (Upper Llandovery–Lower Wenlock) of north-western Mongolia.
 188 Non-figured *M. rozmanae* and *M. sp.* specimens have been reported (Sennikov *et al.*,
 189 2015) from the Aeronian (Middle Llandovery) Sadra section (Gornaya Shoriya, Altai
 190 Republic, Russia) and the Sheinwoodian (Lower Wenlock) Upper Tarkhata
 191 Subformation (Charygka horizon, Gorny Altai, Altai Republic, Russia) and Baytal
 192 Formation (Pichishui Horizon, Tuva Republic, Russia).

193 **Diagnosis**

194 As for the type species.

195

196 **MONGOLEPIS ROZMANAE** Karatajūtė-Talimaa, Novitskaya, Rozman & Sodov, 1990

197 (Figs. 1, 2A–D, 5A–E, 7A–C, 8D)

198 1990 *Mongolepis rozmanae* Karatajūtė-Talimaa, Novitskaya, Rozman & Sodov, figs.

199 2–5, pl. IX.

200 1992 *Mongolepis rozmanae* Karatajūtė-Talimaa & Novitskaya, fig. 2ж, 3.

201 1995 *Mongolepis rozmanae* Karatajūtė-Talimaa, fig. 1.



202 1998 *Mongolepis rozmanae* Karatajūtė-Talimaa, figs. 11, 20.

203

204 **Emended diagnosis**

205 Mongolepidids (pertaining to Mongolepididae) possessing large scales, constricted
 206 along their anterior margin, containing a large number of primary odontocomplex rows
 207 (up to 50+) with long, sigmoidal odontodes. Inter-odontocomplex spaces divided into
 208 pore-like compartments by short, transverse struts. Bulbous base with a prominent
 209 crescent-shaped anterior platform that forms below the level of the crown surface and
 210 extends laterally into two spine-shaped processes.

211 **Holotype**

212 An ontogenetically mature scale  1-031) deposited in collection  of the
 213 Lithuanian Geological Survey, Vilnius (Karatajūtė-Talimaa et al., 1990).

214 **Referred material**

215 Hundreds of isolated scales from the type locality (from samples 16/3 and ЦГЭ
 216 N1009). Non-figured specimens examined for this study are stored in the
 217 microvertebrate research collection of the Lapworth Museum of Geology, University of
 218 Birmingham, UK.

219 **DESCRIPTION**

220 **Morphology**

221 Primary odontodes from the same position in the crown are of equal size irrespective
 222 of scale dimensions. The number of odontocomplex rows changes with the
 223 proportions of the crown and its size, with scales of up to 2 mm in length usually

possessing less than 20 odontocomplexes, whereas in larger specimens their number varies from 20 to c. 35.

Primary odontodes exhibit posteriorly curved profiles and an incremental increase in length towards the posterior of the scale (Figs. 5A, B, 8D). This creates a significant height difference (over five fold in medial odontocomplexes) between the anterior- and the posterior-most elements primary odontodes, whilst odontode thickness remains relatively constant at c. 50 μm (Figs. 5A, B, 8D). The crown surface profile is planar (Fig. 2A, B, D) due to a gradual decrease in the angle of odontode curvature towards the posterior of the scale, accompanied by sloping of the crown/base contact surface (Figs. 5A, 8D).

In scales larger than 1 mm, secondary odontodes are developed to a varying extent along the anterior margin of the crown (Fig. 2A, B, D). These are arranged into rows and are undivided by inter-odontode spaces (Fig. 2A, B, D). Similarly to the main crown odontodes, the secondary odontodes are posteriorly arched elements that demonstrate an unidirectional increase in length (Figs. 5A–B, 8D); the latter being expressed towards the anterior end of the scale.

The scale bases are bulbous structures (Fig. 2A–C) that reach their maximum thickness directly under the anterior apex of the crown. To the posterior, the majority of scale bases display a pitted lower-base surface produced by series of canal openings (Fig. 2B, C).

Histology

245 Scale odontodes are composed of atubular dentine (Fig. 5A–C) for which Karatajūtė-
246 Talimaa et al. (1990) used the term lamellin (first introduced by Bolshakova and
247 Ulitina, 1985). Within individual odontodes, the lamellin displays two histologically
248 distinct regions—a peripheral (10–20 µm thick) lamellar zone and an inner region
249 dominated by mineralised spherites united within *Liesegang* waves (Fig. 5C). The
250 diameter of the calcospherites changes randomly but rarely exceeds 15 µm.

251 Primary odontode pulps are either closed off or can be greatly constricted by
252 dentine infill yet remaining open at their lower end, from which emerges a pair of short
253 (c. 15 µm) horizontal canals that connect the pulp cavity to the odontode surface (Fig.
254 7C, C1). The foramina of these canals face either the inter-odontocomplex spaces or,
255 in marginal odontodes, are exposed at the periphery of the crown (Fig. 2A).

256 In a similar manner to primary odontocomplexes, the pulps of secondary
257 odontodes are substantially constricted by dentine deposition, but they lack the
258 network of horizontal canals (Figs. 2A, B, 7C) developed inside the rest of the crown.

259 The scale base consists of acellular bone characterized by a succession of
260 convex-down growth lamellae (up to 150 µm thick; Fig. 5A, D, 8D) that increase in
261 extent towards the lower portion of the tissue. Secondary lamination is evident within
262 these primary depositional structures and is produced by intrinsic mineralised fibres
263 (*sensu* Ørvig, 1966) of c. 2 µm diameter, which likewise demarcate the boundary
264 surfaces of primary lamellae (Fig. 5D). The basal bone also contains elaborately
265 organised extrinsic crystalline fibres (*sensu* Ørvig, 1966) of c. 2 µm diameter (Fig. 5A,
266 E), which have the appearance of hollow cylindrical rods (Fig. 4E). These are grouped

into layers oriented obliquely with respect to one another (Fig. 5A, E, 8D), that propagate through the tissue. The layers exhibit straight to upwardly arching profiles and thickness of c. 50-70 μm (Fig. 5A, D, E; 8D).

The base houses a vascular system represented by curved (both anteriorly and posteriorly) large-calibre vertical canals (c. 100 μm ; Fig. 7A, B) that are split at their upper end into two or more rami, each merging with one of the primary odontode pulps. Conversely, the secondary odontode pulps are not connected to the canal system of the base.

Remarks

In contrast to earlier work on *Mongolepis* (Karatajūtė-Talimaa et al., 1990; Karatajūtė-Talimaa, 1998), the present study reinterprets the pattern of scale ontogenesis of the genus. Recorded size differences between *Mongolepis* scales have been used by previous authors (Karatajūtė-Talimaa et al., 1990; Karatajūtė-Talimaa, 1998) to identify four distinct ontogenetic stages in the development of the scale cover. They have suggested synchronomorial crown growth succeeded by incremental deposition of basal bone to typify the scale morphogenesis of *Mongolepis*, with scales of ever-increasing crown size and base thickness assumed to be added at each stage of scale cover ontogeny. A re-examination of *Mongolepis* specimens has revealed the presence of bases across the spectrum of documented scale sizes. Furthermore, specimens in the sub-millimetre size category, corresponding to the papillary and juvenile scales of Karatajūtė-Talimaa et al. (1990), possess bases that are proportionally as thick as those of larger scales. Thus, scales interpreted as being

composed exclusively of odontodes (Karatajūtė-Talimaa, 1998, fig. 11A2, E) were related to specimens where the bases had been abraded away. This new morphological evidence supports incremental and mutually synchronous deposition of *Mongolepis* crown and base scale components. The odontocomplex structure and base depositional lamellae of *Mongolepis* scales are similarly identified in all mongolepid genera and indicate that cyclomorial scale growth is a characteristic of the Mongolepidida (refer to Discussion for details).

Genus **TESLEPIS** Karatajūtė-Talimaa & Novitskaya, 1992

Type and only species

Teslepis jucunda Karatajūtė-Talimaa & Novitskaya, 1992, from the Chargat Formation (Salhit regional Stage, Upper Llandovery–Lower Wenlock) of north-western Mongolia. Non-figured *T. jucunda* specimens have been reported (Sennikov et al., 2015) from the Aeronian (Middle Llandovery) Sadra section (Gornaya Shoriya, Altai Republic, Russia) and the Sheinwoodian (Lower Wenlock) Upper Tarkhata Subformation (Charygka horizon, Gorny Altai, Altai Republic, Russia).

Diagnosis

As for the type species.

TESLEPIS JUCUNDA Karatajūtė-Talimaa & Novitskaya, 1992

309 (Figs. 2E–G, 5F, 7D, 8A)

310 1992 *Teslepis jucunda* Karatajūtė-Talimaa & Novitskaya, figs. 1, 2a–e, 3, 4, pl. V figs.
311 1–8.

312 1992 *Teslepis* sp. Karatajūtė-Talimaa & Novitskaya, pl. V fig. 9.

313 1998 *Teslepis jucunda* Karatajūtė-Talimaa, fig. 19.

314 **Emended diagnosis**

315 Mongolepidids with small scales whose odontocomplex number increases with scale
316 size. Non-odontode atubular globular dentine developed at the anterior and lateral
317 crown margins. Scale base extended into an antero-basally directed conical
318 projection.

319 **Holotype**

320 An ontogenetically mature scale (M-1-077) deposited in collection M-1 of the
321 Lithuanian Geological Survey, Vilnius (Karatajūtė-Talimaa & Novitskaya, 1992).

322 **Material**

323 Several hundred of isolated scales from the type locality (from samples 16/3 and ЦГЭ
324 N1009). Non-figured specimens examined for this study are stored in the
325 microvertebrate research collection of the Lapworth Museum of Geology, University of
326 Birmingham, UK.

327

328 **DESCRIPTION**

329 **Morphology**

The number of the scale odontocomplex rows is related to crown size and its proportions. In small specimens (less than 0.5 mm long) their number varies from 4 to 6, whilst it reaches 17 in scales larger than 1 mm. Within the individual odontocomplexes the odontode length gradually increases in a posterior direction (Fig. 5F), whereas odontode thickness remains relatively constant at c. 50 μm .

In the majority of specimens a crescent-shaped platform (Fig. 2E, F) is formed anterior to the odontocomplexes, and the former can be elevated slightly above the level of the odontodes. The absence of this thickening does not correlate with a particular scale size.

The base is not constricted at the contact with the crown (Fig. 2E–G) and extends away from this junction into an anteriorly-directed conical projection that protrudes beyond the crown margin. The posterior third of the base is shallower in comparison with its thickened anterior (Fig. 5F), and is marked by rows of canal openings (30–60 μm in diameter; Fig. 2G) aligned with the odontocomplexes of the crown.

Histology

The crown odontodes consist of atubular dentine (lamellin; Fig. 5F) having a predominately lamellar periphery and an inner spheritically mineralised region. The calcospherites of the globular lamellin attain a diameter of approximately 10 μm and comprise of concentric *Liesegang* rings closed around a central cavity. These exhibit linear or concave arrested growth contact surfaces with other spherites and adjacent *Liesegang* waves. The scale odontodes possess vascular spaces in the form of

vestiges of pulp canals that are mostly filled by lamellin. The pulps branch out laterally as paired short horizontal canals (diameter 10–15 μm) that open on the odontode surface (Fig 7D, D1).

A structural variety of atubular dentine different from lamellin forms the crown platform that surmounts the thickest part of the base (Fig. 5F). This tissue exhibits exclusively spheritic mineralisation represented by tightly packed globules (up to 10 μm in diameter), and lacks a canal system.

The basal bone is acellular with a series of depositional lamellae demarcated by basally arched intrinsic fibres (Fig. 5F). The smallest lamellae reside at the level of the anterior-most odontodes, with lamella thickness varying from 15 μm to 20 μm across the extent of the tissue.

The basal bone contains extrinsic mineralised fibres grouped into 20–40 μm thick layers with upwardly curved profiles. The fibres within each layer are mutually parallel but also oriented obliquely to those of adjacent lamellae, giving the bone a plywood-like texture. In addition to the abundant fibres with layered organization, the tissue contains a set of extrinsic, vertically oriented fibres (Fig. 5F) that are evenly spaced at about 5 μm intervals and propagate up to the level of the crown-base junction.

The base is penetrated by a number of large-calibre vertical vascular canals (Fig. 7D, D1), which connect with the pulp cavities of crown odontodes. The former are predominantly preserved in the posterior (thinnest) third of the base as anteriorly

373 arching canals that gradually widen to c. 40 μm at the lower base surface (Fig. 7D,
374 D1).

375 Remarks

376 The anterior crown platform of *Teslepis* scales (developed also in *Sodolepis*) received
377 little attention in the descriptions of Karatajūtė-Talimaa & Novitskaya (1992) and
378 Karatajūtė-Talimaa (1998), apart from being identified as composed of an
379 undetermined type of globular basal tissue. The platform always forms at the level of
380 the primary odontodes and sutures to the anterior most of them, developing in the
381 space typically occupied by secondary odontodes in *Mongolepis*, *Rongolepis*,
382 *Xinjiangichthys* and *Shiqianolepis* scales. From a histological perspective, the lack of
383 lamellar matrix and the predominantly arrested-growth contact surfaces of spherites
384 resemble the microstructure of certain types of spheritically mineralized dentine
385 (Schmidt & Keil, 1971, fig. 46, 47). Consequently, this tissue is regarded to be globular
386 atubular dentine as opposed to globular dermal bone that is commonly formed only in
387 the cavity-rich cancellous zone of the exoskeleton of lower vertebrates (Ørvig, 1968;
388 Donoghue, Sansom & Downs, 2006; Downs & Donoghue, 2009).

389 Contrasting with the well-defined and consistent shape of the odontodes, the
390 anterior platform has an irregular surface and poorly defined boundaries, and whose
391 shape is determined by the contours of the underlying base. Following on from the
392 above, it could be suggested that this mass of globular dentine is not the product of a
393 well-differentiated dermal papilla, which typifies early odontode development and
394 determines the morphology of odontodes independently of that of the basal bone

(Sire, 1994; Sire & Huysseune, 1996; Sire & Huysseune, 2003). Outside *Teslepis* and *Sodolepis*, dentine structures with similar characteristics have not been documented in the integumentary skeleton of gnathostomes.

Cellular basal bone was considered by Karatajūtė-Talimaa & Novitskaya (1992) to be a diagnostic characteristic of *Teslepis* in the original description of the genus. The fusiform odontocyte lacunae identified in that study are demonstrated here to actually represent the hollow interiors of the mineralised fibres of the bone matrix.

Genus **SODOLEPIS** Karatajūtė-Talimaa & Novitskaya, 1997

Type and only species

Sodolepis lucens Karatajūtė-Talimaa & Novitskaya, 1997, from the Chargat Formation (Salhit regional Stage, Upper Llandovery–Lower Wenlock) of north-western Mongolia.

Diagnosis

As for the type species.

SODOLEPIS LUCENS Karatajūtė-Talimaa & Novitskaya, 1997

(Figs. 2H–J, 5G–J, 7E)

1997 *Sodolepis lucens* Karatajūtė-Talimaa & Novitskaya, figs. 1–3, pl. XI.

1998 *Sodolepis lucens* Karatajūtė-Talimaa, fig. 18.

Emended diagnosis

Mongolepidids with medium scales possessing crowns composed of sutured odontocomplex rows, whose number does not increase with scale size. Anterior crown platform of globular dentine elevated to the level of the crown surface. Neck (horizontal) canals not formed at the lower portion of crown odontodes.

Holotype

An isolated scale with accession number  M-1-091 deposited in collection  M-1 of the Lithuanian Geological Survey, Vilnius (Karatajūtė-Talimaa & Novitskaya, 1997).

Referred material

More than a hundred isolated scales from the type locality (samples 16/3 and $\text{L}\Gamma\Theta$ N1009). Non-figured specimens examined for this study are stored in the Lapworth Museum of Geology, University of Birmingham, UK.

Remarks

The gross morphology of *Sodolepis* scales (Fig. 2H–J) closely resembles that of *Teslepis*, with the two genera demonstrating comparable histology. The latter, however, are distinguished on the basis of differences in odontode size and crown vascularization. *Sodolepis* crowns possess fused odontocomplexes, composed of odontodes that are on average three times as large of those of *Teslepis*, divided by inter-odontocomplex spaces. This is due to a corresponding increase of odontode and scale size in *Sodolepis*, leading to the formation of a relatively constant number of

odontocomplexes irrespective of crown dimensions. In *Teslepis* specimens, on the other hand, odontode size remains consistent across all documented scale lengths.

As noted by Karatajūtė-Talimaa & Novitskaya (1997), a system of horizontal canals cannot be identified inside *Sodolepis* scale crowns (Fig. 7E)—an atypical condition considering that the majority of mongolepid genera, including *Teslepis*, develop some type of pulp canal openings on the lower crown surface.

Genus ***RONGOLEPIS*** Sansom, Aldridge & Smith, 2000

Type and only species

Rongolepis cosmetica from the Telychian (Upper Llandovery) of south China, Lower Member of the Xiushan Formation (Sansom, Aldridge & Smith, 2000) and the Telychian of Bachu County, Xinjiang, China (Lower member of the Yimugantawu Formation; N-Z Wang, unpublished data).

Diagnosis

As for the type species.

RONGOLEPIS COSMETICA Sansom, Aldridge & Smith, 2000

(Figs. 2K–M, 5K, L)

2000 *Rongolepis cosmetica* Sansom, Aldridge & Smith, figs. 11, 12.

Emended diagnosis

Mongolepidid species with scale odontocomplex rows ornamented by narrow median ridges, flanked anteriorly and laterally by conical secondary odontodes. Posterior primary odontodes long and straight, having pitted by rows of foramina on their lower crown face. Base tetragonal or oblong, displaced towards the scale anterior. Lower base surface concave to flat with a central conical projection.

Holotype

An isolated scale (NIGP 130326) from the Xiushan Formation of south China (Sansom, Aldridge & Smith, 2000).

Referred material

Hundreds of specimens from the Xiushan Formation of Leijiatun (Shiqian county, south China (sample Shiqian 14B), including type series material (NIGP 130319–NIGP 130330) figured by Sansom, Aldridge & Smith (2000). Non-figured specimens stored in the Nanjing Institute of Geology and Palaeontology, Chinese Academy of Sciences, Nanjing, China.

Remarks

The uncertainty regarding the supergeneric position of *Rongolepis* in the original description of the genus (Sansom, Aldridge & Smith, 2000) has been attributed to a suite of characteristics (scale morphology, posterior of the crown composed of acellular lamellar bone and presence of crown odontodes) not known in the scales of

other vertebrates. The re-examination of *Rongolepis cosmetica* has enabled the identification of a combination of features diagnostic for Mongolepidida. Of particular importance in this regard is the nature of the tissue composing the flared posterior extension of *Rongolepis* scales. Suggested to be formed of lamellar bone (Sansom *et al.* 2000), this portion of the scale in fact demonstrates the lamellin-type architecture of an **ionotropically** and spheritically mineralised atubular tissue devoid of attachment fibres (Fig. 5K, L). Moreover, the segmentation of the crown's posterior part observed in thin sections (Fig. 5K, L; Sansom, Aldridge & Smith, 2000, fig. 12e) is interpreted to be produced by the contact surfaces of sutured odontodes. Both the anterior to posterior increase in length of these elements and their arrangement in longitudinal rows over the posterior half of the base are known features of mongolepid primary odontocomplexes. The assignment of *Rongolepis* to Mongolepidida is thus dictated by the possession of its scales of lamellin and polyodontocomplex growing crowns.

Family **SHIQIANOLEPIDAE** Sansom, Aldridge & Smith 2000

Included Genera

Xinjiangichthys Wang et al., 1998 and *Shiqianolepis* Sansom, Aldridge & Smith, 2000.

Emended diagnosis

Mongolepids with scale bases composed of non-vascular, cellular bone tissue.

493 Genus **SHIQIANOLEPIS** Sansom, Aldridge & Smith, 2000

494 **Type and only species**

495 *Shiqianolepis hollandi* Sansom, Aldridge & Smith, 2000, from the Telychian Lower
496 Member of the Xiushan Formation (Leijiatusun, Shiqian county, southern China).

497 **Emended diagnosis**

498 As for the type species.

499

500 **SHIQIANOLEPIS HOLLANDI** Sansom, Aldridge & Smith, 2000

501 (Figs. 3A–C, 4N, 7F, 8B, E)

502 2000 *Shiqianolepis hollandi* Sansom, Aldridge & Smith, figs. 4–6.

503 **Emended diagnosis**

504 Shiqianolepids with trunk scale odontocomplexes separated posteriorly by deep inter-
505 odontocomplex spaces. A cluster of tightly sutured secondary odontodes formed
506 anteriorly of crown odontocomplexes. Crown surface ornamented by tuberculate
507 ridges. Oblong asymmetrical head scales (up to 1 mm long) with irregularly-shaped
508 odontodes distributed peripherally around a medial ridge.

509 **Holotype**

510 An isolated trunk scale (NIGP 130294) from the Xiushan Formation of Leijiatusun (Shiqian

County) south China (Sansom, Aldridge & Smith, 2000).

Referred material

Hundreds of isolated scales and type series specimens (NIGP 130293–NIGP 130318) figured by Sansom, Aldridge & Smith (2000) from the Telychian Xiushan Formation (sample Shiqian 14B) of Leijiatun (Shiqian county, south China). Non-figured material stored in the Nanjing Institute of Geology and Palaeontology, Chinese Academy of Sciences, Nanjing, China.

Remarks

Characteristic for *Shiqianolepis* scales is a distinct primordial odontode located at the apex of the conical base. This odontode has been termed ‘proto-scale’ by Sansom, Aldridge & Smith (2000) and was identified as a diminutive element overlain by the much larger odontodes deposited at later stages of crown ontogeny. Superpositional growth, which results in odontodes not being exposed on the crown surface, is a condition atypical for other mongolepids, also demonstrated to not be a feature of *Shiqianolepis* scales. Upon re-examination of figured material and newly sectioned specimens, the primordial odontode borders recognized in Sansom, Aldridge & Smith (2000, figs. 6b, 7) are now considered to constitute the margins of dentine depositional lamellae (Fig. 5N), as these are occasionally observed to be indented by more peripherally formed calcospherites—evidencing a centripetal mode of dentine histogenesis as opposed to stacking of primary odontodes. As identified here, the primordial odontode in *Shiqianolepis* scales is overlapped only at its anterior end by secondary odontodes, whilst most of its upper margin remains exposed on the crown

surface. Similarly to the rest of the odontocomplexes of *Shiqianolepis* trunk scales, the one incepted by the 'proto-scale' also displays a gradual posterior increase of odontode size.

Genus **XINJIANGICHTHYS** Wang, Zhang, Wang & Zhu, 1998

Type and only species

Xinjiangichthys pluridentatus Wang, Zhang, Wang & Zhu, 1998, from the Telychian Yimugantawu Formation (north-western margin of the Tarim Basin, Xinjiang, PR China).

Emended diagnosis

As for the type species.

Remarks

The placement of *Xinjiangichthys* inside Mongolepidida by Wang et al. (1998) was justified on the grounds of similarities in crown morphology and odontode patterning with Mongolian mongolepids (the only known mongolepid taxa at the time of its description), and this study advances that claim further by identifying a polyodontocomplex crown structure in *Xinjiangichthys* scales.

The presence of atubular dentine in *Xinjiangichthys* scales, another of the diagnostic characters of mongolepids (this study; Karatajūtė-Talimaa et al., 1990;

Sansom, Aldridge & Smith, 2000), can be determined in thin-section (Fig. 5M) and through X-ray microtomography (Fig 7G, H).

Furthermore, Wang et al.'s (1998) interpretation of *Xinjiangichthys* scale bases as non-growing is rejected here by the recognition of a conical basal tissue that supports, at its apex, the primordial odontode and further posteriorly the rest of the scale's primary odontodes, similarly to the growing bases of *Shiqianolepis* and those of mongolepids in large (Fig. 5M; Fig. 7H).

XINJIANGICHTHYS PLURIDENTATUS Wang, Zhang, Wang & Zhu, 1998

(Figs. 3D–F, 5M, 7G–H)

1998 *Xinjiangichthys pluridentatus* Wang, Zhang, Wang and Zhu, pl. 1, fig. a–d.

1998 *Xinjiangichthys tarimensis* Wang, Zhang, Wang & Zhu, pl. 1, fig. e–i.

v. 2000 *Xinjiangichthys* sp. Sansom, Aldridge and Smith, 236, fig. 8.

Emended diagnosis

Shiqianolepids with unornamented scale crowns composed of sutured odontocomplex rows. Needle-like primary odontodes; erect, conical secondary odontodes.

Holotype

An isolated trunk scale (IVPP V11663.1) from the Yimugantawu Formation of Xinjiang (Bachu county), China (Wang et al., 1998).

Referred material

Two specimens from the Telychian Xiushan Formation (Leijiatusun, Shiqian county, south China; sample Shiqian 14B), in addition to material figured (NIGP 130291, NIGP 130292) in Sansom, Aldridge & Smith (2000), and five specimens (including IVPP V X1, IVPP V X2) from the Yimugantawu Formation (Bachu county, Xinjiang, PR China). Non-figured scales are stored in the Nanjing Institute of Geology and Palaeontology, Chinese Academy of Sciences, Nanjing, China and the Institute of Vertebrate Paleontology and Paleoanthropology, Chinese Academy of Sciences, Beijing, China.

Remarks

X. tarimensis and *X. sp.* are synonymised with *X. pluridentatus* based on the absence of differentiating characteristics between the specimens attributed to the two species. The arguments (equal-sized crown odontodes, scale neck and pitted sub-crown surface) of Wang et al. (1998) for erecting *X. tarimensis* are considered not valid for the following reasons. The large-diameter anterior odontodes of *X. pluridentatus* specimens figured by Wang et al. (1998, pl. 1a, c) represent secondary odontodes not developed in all scales of the species (specimens identified as *X. tarimensis* by Wang et al., 1998, pl. 1e-i), which is consistent with the condition documented in *Mongolepis* (this study and Karatajūtė-Talimaa et al., 1990). The presence of secondary odontodes also accounts for the lack of a distinct neck in the *Xinjiangichthys* scales they develop, by occupying the sloped anterior surface of the base. The third character considered diagnostic for *X. tarimensis* by Wang et al. (1998) are the

numerous foramina present on the lower crown surface of scales, which are also seen (Figs. 3D, E, 7G–H) in *Xinjiangichthys* specimens with secondary odontodes.

Family *incertae sedis*

Genus ***SOLINALEPIS*** gen. nov.

Type and only species

Solinalepis levis gen. et sp. nov.

Derivation of name

From ‘solinas’ (tube, pipe in Greek), pertaining to the shape of the scale odontodes of the species, and ‘lepis’, scale in Greek.

Diagnosis

As for the type species.

Remarks

Characters relating to the dimensions of the scale base (its length and thickness in relation to those of the crown) unite *Solinalepis* gen. nov. (data from yet to be published phylogenetic analysis by Andreev *et al.*) in a clade with members of Shiqianolepidae. Nevertheless, this type of morphological data is not regarded informative at a supra-generic level and the genus is classified outside the two recognized mongolepid Families due to differences in scale base histology (acellular

bone lacking plywood-like organization of its mineralised matrix). As a consequence,
Solinalepis gen. nov. is treated as *Mongolepidida incertae sedis*.

SOLINALEPIS LEVIS sp. nov

(Figs. 4, 6, 7I–J, 8C)

2001 ‘?Mongolepid scales’ Sansom, Smith and Smith, p. 161, fig. 10.3g, h.

2002 Unnamed chondrichthyan Donoghue and Sansom, p. 362, fig. 6.3.

2009 Stem-chondrichthyan Sire, Donoghue and Vickaryous, p. 424, fig. 10c.

Derivation of name

From the Latin ‘levis’ (smooth), referring to the unornamented scale crown surface of
the species.

Locality and horizon

The type locality is the vicinity of the Harding Quarry, situated c. 1 km west of Cañon
City (Fremont County, Colorado, USA). All *Solinalepis* specimens come from
Sandbian strata (Mohawkian regional series, *Phragmodus undatus* conodont zone) of
the Harding Sandstone (samples H94-26 and H96-20).

Holotype

An isolated trunk scale BU5310 (Fig. 4E).

Referred material

Hundreds of isolated scales, including BU5307–BU5318, BU5345. Non-figured specimens examined for this study are stored in the microvertebrate research collection of the Lapworth Museum of Geology, University of Birmingham, UK.

Diagnosis

Mongolepid species with trunk scales crowns composed of tubular odontodes organized in sutured longitudinal odontocomplex rows. Acellular basal bone housing an elaborate canal system that opens via foramina on the basal surface. Radially arranged tuberculate to conical head-scale odontodes.

DESCRIPTION

Morphology of trunk scales

The length of these scales varies between 100–400 μm and is always less (up to three quarters) than their width. Specimens with crown lengths near or exceeding 200 μm demonstrate polygonal (Fig. 4E–G), often asymmetrical (Fig. 4F, G), outlines. The anterior crown margin of these scales is typically wedge-shaped whilst their posterior face is straight (Fig. 4I). In contrast, the crowns of antero-posteriorly short (100–200 μm long) scales tend to be symmetrical, leaf-shaped structures (Fig. 4J–L), rarely demonstrating simple geometrical profiles in crown view.

Irrespective of crown morphology, the odontodes of trunk scales are organized into closely packed antero-posteriorly aligned rows (Figs 4F–G, J, 8C). Adjacent rows

are displaced by approximately half an odontode diameter (c. 15 μm), resulting in an offset between the odontodes of neighbouring odontocomplexes (Fig. 8C). The odontodes themselves are cylindrical, tube-like elements with sigmoidal profiles that taper to a point apically (Fig. 4J). Odontode length increases gradually towards the scale's posterior end, where the crown can reach a height of c. 400 μm .

The crown/base transition is not marked by a neck-like constriction (Fig. 4E–L), with the base never attaining more than a third of the overall scale height. The basal surface is typically marked by deeply incised grooves (Fig. 4E–I) that give it a dimpled appearance, characteristic also for the lower base surface. The latter has a predominantly flat profile but can exhibit a central conical projection that is particularly well developed in leaf-shaped specimens (Fig. 4L).

Morphology of head scales

Polyodontode symmetrical or asymmetrical scales with height between 0.5 and 1.3 mm. These are represented by two main morphological variants, a compact, bulbous type (Fig. 4D) and tessera-like scales (Fig. 4A–C) of larger diameter. Both morphotypes possess irregular crowns composed of radially ordered odontodes, and do not clearly exhibit distinct anterior, posterior and lateral scale faces. The radiating odontodes form rows (five to nine odontodes long), offset in a manner in which the odontodes of each row oppose the inter-odontode contacts of neighbouring odontocomplexes. Odontode height diminishes gradually towards the crown centre, accompanied by an increase of coalescence between odontodes.

The scales exhibit a prominent central bulge, away from which the crown surface slopes down to the scale margin. In crown view, the latter has a corrugated outline that in certain specimens is accentuated by deep, peripherally expanding grooves (Fig. 4A, B).

The scale base displays a granular, grooved surface and follows the outline of the crown. At its centre the base attains maximal thickness (Fig. 6A), and gradually decreases in height away from this point. The lower-base surface is predominantly planar or can have a moderate central concavity, but never exhibits the convex topology documented in trunk scale specimens.

Histology of trunk scales

Crown odontodes are structured out of atubular dentine (lamellin; Fig. 6B) that is spherically mineralised in proximity of the pulp (spherite diameter 10–15 μm).

Cylindrical, non-branching pulp cavities occupy the centre of odontodes and are connected at their lower ends with the canal system of the base (Fig. 7I, J). The latter is represented by vertical canals that bifurcate close to the crown-base junction, with each pair of rami re-connecting deeper inside the base, resulting in the formation of a series of vascular loops (Fig. 7I, J). Vertically oriented canals emerge from the looped canal system and open on the lower base surface. The basal surface is similarly marked by numerous foramina that are the exit points for the peripheral canals of the base (Fig. 4H).

The base is composed of acellular bone demonstrating the presence of c. 2 μ m thick extrinsic crystalline mineralised fibres that propagate vertically through the tissue (Fig. 6B).

Histology of head scales

Due to diagenetic alteration of histologically examined scales, the microstructure of crown odontodes is largely obscured. Nevertheless, wide odontode pulp canals are evident in sectioned specimens (Fig. 6A), and these appear to end blindly inside the crown. The upper base surface is perforated by a row of foramina (Fig. 4C, D) similar to the ones documented in trunk scales.

The main structural components of the basal bone matrix are tightly packed, parallel crystalline mineralized fibres with horizontal orientation (Fig. 6A). These are crosscut by apically converging fibre bundles (up to 15 μ m in diameter), which follow undulating paths across the tissue.

Remarks

The development of polyodontocomplex scale crowns formed from lamellin identify *Solinalepis levis* gen. et sp. nov. scales as a mongolepid species. Moreover, the trunk scale odontocomplexes of *Solinalepis* gen. nov. exhibit the same progressive posterior increase in odontode length documented in members of the Order.

Within Mongolepidida, the combination of a large odontocomplex number (>20) and sutured odontodes is present only in the Telychian genus *Xinjiangichthys*. Nevertheless, the two taxa are readily distinguished on the basis of base histology and

canal-opening distribution on the scale surface. In addition to that, *Solinalepis* gen. nov. is one of only two described mongolepid genera (the other being *Shiqianolepis*) known to develop with squamation clearly differentiated into distinct trunk (exhibiting recognizable anterior and posterior faces) and head morphotypes (irregular-shaped elements)—a condition that is consistent with that recorded in a number of heterosquamous Lower Palaeozoic gnathostomes known from articulated specimens (e.g. *Climatius reticulatus* Miles, 1973, *Obtusacanthus corroconius* Hanke & Wilson, 2004, *Gladiobrachius probaton* Hanke & Davis, 2008 and *Ptomacanthus anglicus* Miles, 1973; Brazeau, 2012).

DISCUSSION

Crown morphogenesis of mongolepid scales

Shiqianolepis hollandi is recognized as a key taxon for determining the mode of scale crown development in mongolepids, following the identification by Sansom, Aldridge & Smith (2000) of ‘proto-scale’ (early-development phase) specimens of the species (Sansom, Aldridge & Smith, 2000, fig. 4u, w). The size (half of that of ‘mature’ trunk scales) and the small number of crown odontodes (exhibiting only the earliest formed odontodes of incipient primary odontocomplexes) of these scales implies that in *Shiqianolepis* scale ontogenesis involves crown enlargement through sequential addition of odontodes. Significantly, this style of crown architecture (primary odontocomplex rows originating at the most elevated point of the base and characterized by a posterior increase in size of their constituent odontodes) is

developed in all members of the Mongolepidida (Figs. 5A, F, I, K, M, N, 8) and is evidence that the mongolepids share a cyclomorior pattern of scale ontogenesis.

Data from developmental studies on extant neoselachians indicate that their scales cannot serve as model systems for determining the mechanism of morphogenesis of the compound mongolepid scale crowns, as the former have been shown to be simple mono-odontode elements produced by a single epithelio-ectomesenchymal primordium (Schmidt & Keil, 1971; Reif, 1980, Miyake et al., 1999; Sire & Huysseune, 2003; Johanson, Smith & Joss, 2007; Johanson et al., 2008). Examinations of multiple odontode generation in osteichthyan scales (Kerr, 1952; Smith, Hobdell & Miller, 1972; Smith, 1979; Sire & Huysseune, 1996), though, provide insight into the timing of deposition of odontode aggregations associated with a dermal bone support tissue. They reveal phases of odontode generation that result in an increase of odontode number throughout scale ontogeny.

The proposed here scale growth mechanism in Mongolepidida is further substantiated by evidence from the Palaeozoic record of the Chondrichthyes. The scale crown structure of certain chondrichthyan taxa described from articulated specimens (e.g. *Diplodoselache woodi* Dick, 1981, *Tamiobatis vetustus* Williams, 1998 and *Orodus greggi* Zangerl, 1968), conform closely to the odontode patterning of mongolepid scales. *Diplodeselache* trunk scales were noted by Dick (1981) to closely resemble those of *Orodus* and to be similarly characterized by cyclomorior growth. Previous work (Reif, 1978) on the morphogenesis of the chondrichthyan integumentary skeleton also recognized sequential crown elongation through regular addition of odontodes as the mechanism of scale development in *Orodus*. This pattern

of crown formation is also typical for scales with a *Ctenacanthus costellatus* type of morphogenesis (defined by Reif, 1978 and equivalent to the *Ctenacanthus* B3 morphogenetic type of Karatajūtė-Talimaa, 1992) to which *Tamiobatis* scales have been attributed (Williams, 1998).

Mongolepid scale crown histology

The emergence of skeletal mineralisation in vertebrates (Donoghue & Sansom, 2002; Donoghue, Sansom & Downs, 2006) coincides with the origin of the phylogenetically most primitive atubular dentine-like tissues that compose the basal bodies of certain conodont genera (Sansom, 1996; Smith, Sansom & Smith, 1996; Donoghue, 1998; Dong, Donoghue & Repetski, 2005). Conodont atubular ‘dentines’ frequently exhibit (Sansom 1996, fig. 2e–h; Donoghue, 1998, fig. 5a–c; Dong, Donoghue & Repetski, 2005, pl. 1, figs 3–9) peripheral lamellar fabric, substituted internally by spherically mineralised matrix, making them comparable with the architecture of mongolepid lamellin (Fig. 5C, G). This structure has recently been proposed to have arisen in a stepwise manner in the oropharyngeal skeleton of Paraconodonta and Euconodonta (Murdock et al., 2013), and within Gnathostomata the known occurrence of atubular dentines outside the Mongolepidida is limited to the scale odontodes of the pteraspidomorph *Tesakoviaspis concentrica* (Karatajūtė-Talimaa & Smith, 2004) and the fin spine ornament of sinacanthid gnathostomes (Sansom, Aldridge & Smith, 2000; Sansom, Wang & Smith, 2005).

An important aspect of the atubular nature of lamellin is that it provides circumstantial evidence for the involvement of atypical (from a modern perspective) odontoblasts in

the generation of the tissue. During dentinogenesis mature odontoblasts commonly extend long cellular processes into the mineralised phase, which remain contained inside tubular spaces after formation of the tissue is complete (Linde, 1989; Linde & Lundgren, 1995; Yoshida et al., 2002; Magloire et al., 2004, 2009). The inability of secretory odontoblasts to form dentinal tubules is taken to suggest that such cells either did not embed their processes within the dentine matrix at any depth or lacked processes altogether. Atypical odontoblasts devoid of large cytoplasmic projections have been reported in the tooth germs of the Recent sting ray *Dasyatis akajei* (Sasagawa, 1995), but these are found to co-exist with unipolar odontoblasts, characterized by well-developed processes. The apical portions of odontoblasts and their processes have been implicated as ion channel-rich sites capable of being activated by environmental stimuli via tubular fluid movement, and are presumably involved in transmitting sensory input to pulp nerve endings (Okumura et al., 2005; Allard et al., 2006; Magloire et al., 2009). This raises the possibility that mongolepid scale pulps had limited ability to transduce sensory input compared with an odontoblast population that forms tubular network inside a mineralised dentine matrix.

Histology of mongolepid scale bases

This and previous studies (Karatajūtė-Talimaa et al., 1990, Karatajūtė-Talimaa & Novitskaya, 1992, 1997; Sansom, Aldridge & Smith, 2000) identify mongolepid scale odontodes to be supported by a common base composed of lamellar bone (Fig. 5A, F, H, I, K, M, N, 6). The basal tissue of *Mongolepis* and *Sodolepis* scales has been interpreted as acellular bone (Karatajūtė-Talimaa et al., 1990; Karatajūtė-Talimaa & Novitskaya, 1997), with this study also recognizing the absence of osteocyte lacunae

in the bases of *Teslepis* (*contra* Karatajūtė-Talimaa & Novitskaya, 1992), *Rongolepis* (in agreement with Sansom, Aldridge & Smith, 2000) and *Solinalepis* gen. nov.—restricting the occurrence of cellular bone inside Mongolepidida to the genera *Xinjiangichthys* and *Shiqianolepis* (this study and Sansom, Aldridge & Smith, 2000).

A plywood-like layering of crystalline fibres is recognized as the predominant type of basal bone texture of mongolepid scales, being documented in the four genera of the Family Mongolepididae. This architecture of the mineralised matrix matches closely the organization of the collagen fibres in the deep dermis (stratum compactum) of extant neoselachians (Motta 1977; Miyake et al., 1999; Sire & Huysseune, 2003) and osteichthyans (Kerr, 1952, 1955; Sire, 1993; Gemballa & Bartsch, 2002) and is suggested to be indicative of dermal bone histogenesis achieved through mineralisation of the a largely unmodified fibrous scaffold of the stratum compactum—a process referred to as metaplastic ossification (Sire, 1993; Sire, Donoghue & Vickaryous, 2009). Consequently, the observed absence of plywood-like layering in the cellular bone of mongolepid scale bases (in *Xinjiangichthys*, *Shiqianolepis* and *Solinalepis* gen. nov.) could be interpreted to result from remodelling of the original fibrous framework of stratum compactum prior to tissue mineralisation (a process described by Sire 1993 in the scales of the armoured catfish *Corydoras arcuatus*).

The data above allow the identification of the site of basal bone formation of mongolepid scales within the deep tiers of the corium, with the tissue being considered to periodically increase in size due to the growth increments documented in sectioned specimens. These depositional phases reveal a common pattern of generation of mongolepid scale bases, wherein each newly laid down lamella covers

the lower surface of the previously deposited one. The geometry of the lamellae shows little change, implying retention of a fairly consistent base shape throughout scale ontogeny. Such a pattern of base morphogenesis is not unique to the Mongolepidida, but appears to be the prevalent mode of bone tissue growth in the scales of jawed gnathostomes, being demonstrated in ‘placoderms’ (Burrow & Turner, 1998, 1999), ‘acanthodians’ (Denison, 1979), basal osteichthyans (Gross, 1968; Schultze, 1968) and early chondrichthyans (Karatajūtė-Talimaa, 1973; Mader, 1986; Wang, 1993).

Canal system of mongolepid scales

Previously, the internal canal system architecture of mongolepid scales had been investigated in detail only in *Mongolepis*, *Teslepis* and *Sodolepis* through oil immersion studies and thin section work (Karatajūtė-Talimaa et al., 1990; Karatajūtė-Talimaa & Novitskaya, 1992, 1997). The employment of X-ray microtomography extended to these observations by enabling visualization of the three-dimensional structure of scale cavity spaces in the examined genera with greater accuracy.

In *Mongolepis*, *Teslepis*, *Sodolepis* and *Solinalepis* gen. nov. the lower ends of odontode pulp cavities are continuous with the canal system of the base. Comparable vascularization is developed in the Upper Ordovician chondrichthyan scale species *Tezakia hardingensis* from North America (Andreev et al. 2015). The lower base surface of this taxon has been demonstrated to exhibit rows of foramina (Sansom, Smith & Smith, 1996, fig. 2a) that are similar to the basal canal openings of mongolepids. Likewise, the central canal of the basal bone tissue is continuous with

the odontode pulp in the Silurian scale genera *Elegestolepis* (Karatajūtė-Talimaa, 1973; Andreev et al., submitted) and *Kannathalepis* (Märss & Gagnier, 2001), which are the earliest recorded mono-odontode scale taxa attributed to the Chondrichthyes (Andreev et al., submitted). This condition is also identified in the mono-odontode scales of various Upper Palaeozoic chondrichthyans (e.g. *Janassa* Ørvig, 1966; Malzahn, 1968, *Ornithoprion* Zangerl, 1966 and *Hopleacanthus* Schaumburg, 1982), Mesozoic hybodonts (Reif, 1978) and extant neoselachians (Reif, 1980; Miyake et al., 1999; Johanson et al., 2008).

Xinjiangichthys, *Shiqianolepis* and *Rongolepis* differ from the other mongolepid genera in having their entire scale canal system confined to the crown, with the lower ends of odontode pulps opening at the crown surface in proximity of the base. The posterior peripheral odontodes of these three genera display additional cavities that are detected as foramina on the lower crown face. A similarly pitted lower crown surface has also been identified in poracanthodid ‘acanthodians’ (Gross 1956; Valiukevičius, 1992; Burrow, 2003), the putative stem chondrichthyan *Seretolepis* (Hanke & Wilson, 2010; Martínez-Pérez et al., 2010), and in ctenacanthiform scales (e.g. *Tamiobatis vetustus* Williams, 1998 and *Ctenacanthus costellatus* Reif, 1978). In the scales of *Poracanthodes* these openings represent the posterior exit points of a complex canal network that is absent from mongolepid scale crowns.

Studies on the squamation of jawed gnathostomes reveal the lack of basal tissue vascularisation to be a common feature of many ‘acanthodians’ (Denison, 1979; Karatajūtė-Talimaa & Smith, 2003; Valiukevičius, 2003; Valiukevičius & Burrow, 2005) and chondrichthyans such as *Protacrodus* (Gross, 1973), *Orodus* (Zangerl, 1968) and

Holmesella (Ørvig, 1966), including some of the earliest known post-Silurian putative chondrichthyan scale taxa (*Iberolepis*, *Lunalepis* Mader, 1986 and *Nogueralespis* Wang, 1993).

Despite the observed differences in canal architecture, all mongolepid genera with the exception of *Sodolepis* develop canal openings exposed on the scale surface in the region the crown-base interface. These foramina represent the termini of canals homologous to the neck canals of euselachians (*sensu* Reif, 1978), as they similarly link the main pulp canal to the odontode surface. In *Mongolepis* and *Teslepis* this connection is established via one pair of short canals (the 'horizontal canals' of Karatajūtė-Talimaa et al., 1990, Karatajūtė-Talimaa & Novitskaya, 1992 and Karatajūtė-Talimaa, 1998) that issue from the lower end of each pulp. The data presented here indicate that the horizontal canal system of these two genera is housed inside the scale crown, contrary to previous depictions of the feature at the crown-base junction (Karatajūtė-Talimaa, 1995, 1998). In contrast, the lower ends of odontode pulp canals of North American and Chinese mongolepids do not branch out, and either continue inside the base without being exposed on the crown surface (*Solinalespis* gen. nov.) or open directly onto it (*Shiqianolepis* and *Rongolepis*).

Systematic position of the Mongolepidida

Recent phylogenies of Palaeozoic gnathostomes incorporate only a limited set of scale characters (Brazeau, 2009; Davis, Finarelli & Coates, 2012; Zhu et al., 2013; Giles, Friedman & Brazeau, 2015), and this is also true for cladistic investigations of the total group Chondrichthyes (Lund & Grogan, 1997; Grogan & Lund, 2008; Grogan,

Lund & Greenfest-Allen, 2012), to which mongolepids have been tentatively suggested to belong (Karatajūtė-Talimaa & Novitskaya, 1997; Sansom, Aldridge & Smith, 2000), that give preference to dental over scale characteristics. Accordingly, chondrichthyans clades have largely been erected based upon tooth characters (Zangerl, 1981; Stahl, 1999; Ginter, Hampe & Duffin, 2010), whereas the position of Lower Palaeozoic shark-like scale taxa has yet to be resolved in phylogenetic hypotheses for the Chondrichthyes.

The coherence of the Mongolepidida is reaffirmed here on the basis of an amended character set, which diagnoses the Order by the unique combination of scale growth, polyodontocomplex scale crowns and development of lamellin. The placement of mongolepids within Chondrichthyes, on the other hand, has been questioned in the past on the basis of their atubular dentine (lamellin) crowns and the presence of a horizontal canal system (Karatajūtė-Talimaa & Novitskaya, 1992). This study suggests that the horizontal canals of *Mongolepis* and *Teslepis* are equivalent to euselachian neck canals, whilst revealing similar canal spaces in the crown odontodes of Chinese mongolepids. However, neck-like canals are likewise also known in the scales of ‘placoderms’ (Burrow & Turner, 1998) and basal Palaeozoic osteichthyans (Gross, 1953, 1968), and are thus not a chondrichthyan apomorphy. Also, scale dentine histology appears to vary greatly within the total group Chondrichthyes (e.g. distinct dentine types are developed in *Elegestolepis* Karatajūtė-Talimaa, 1973, *Seretolepis* Hanke and Wilson 2010, *Orodus* Zangerl, 1968 and *Hybodus* Reif, 1978), which makes it a poor diagnostic character at a supra-ordinal level. By the same token, although atubular dentine occurs in the Mongolepidida, it is also formed in the

dermal skeleton of pteraspidomorph agnathans (Karatajūtė-Talimaa & Smith, 2004) and therefore is uninformative with respect to the relationships of the Order. The systematic affinities of Mongolepidida are determined instead by a unique combination of scale attributes that are shared with other Palaeozoic chondrichthyan lineages. Reference is made here to the *Ctenacanthus*-type squamation of certain xenacanthiform (*Diplodoselache* Dick, 1981), orodontiform (*Orodus* Zangerl, 1968) and cladodontomorph (e.g. *Cladolepis* Burrow, Turner & Wang, 2000 and *Caladoselache* Dean, 1909; P. Andreev pers. obs.) chondrichthyans, characterized by the development of symmetrical trunk scales with multiple crown odontocomplexes that lack cancellous bone, enamel and hard tissue resorption.

CONCLUSIONS

The present revision of Mongolepidida established the Order as a natural group of early chondrichthyans characterized by polyodontocomplex growing scales with *Ctenacanthus*-like crown architecture. However, in agreement with Karatajūtė-Talimaa (1992), the scales of mongolepids are recognized to exhibit a distinct, *Mongolepis*, type of morphogenesis, on account of their lamellin composed crowns.

The description of the mongolepid genus *Solinalepis* gen. nov. from the Sandbian of North America, pushes back the first appearance of the Mongolepidida by 20 My and firmly places the origin of the Chondrichthyes in the Ordovician. Together with reports of other shark-like scale taxa from the Ordovician (Sansom, Smith & Smith, 1996; Sansom, Smith & Smith, 2001; Sansom et al., 2012), this lends further

support to an early chondrichthyan diversification event (proposed by Karatajūtė-Talimaa, 1992), that preceded the first known appearance of chondrichthyan teeth and articulated skeletal remains in the Lower Devonian.

ACKNOWLEDGEMENTS

Solinalepis material was collected from the Harding Sandstone during fieldwork undertaken as part of Natural Environment Research Council Grants GR3/8543 and NER/B/S/2000/0028 awarded to M. Paul Smith (Oxford) and Moya Smith (King's College, London), and we are grateful to both for discussions on the nature of these specimens over the years, whilst specimens of *Shiqianolepis* were made available for study by Richard J. Aldridge (Leicester). Rachel Sammons and Michael Sandholzer provided technical assistance during SEM and micro-CT imaging of mongolepid scales at the School of Dentistry, University of Birmingham.

The present research received support from the Small Grant Awards AGM 2011 (Sylvester-Bradley Award) of the Palaeontological Association, and the School of Geography, Earth and Environmental Sciences of the University of Birmingham, which funded PA via a Doctoral Studentship.

957

958 REFERENCES

- 959 **Allard B, Magloire H, Couble ML, Maurin JC, Bleicher F. 2006.** Voltage-gated
 960 Sodium Channels Confer Excitability to Human Odontoblasts. *Journal of Biological*
 961 *Chemistry* **281**:29002–29010.
- 962 **Andreev PS, Coates MI, Shelton RM, Cooper PR, Smith MP, Sansom IJ. 2015.**
 963 Upper Ordovician chondrichthyan-like scales from North America. *Palaeontology*
 964 **58**:691–704.
- 965 **Andreev PS, Coates MI, Karatajūtė-Talimaa V, Shelton RM, Cooper PR, Sansom IJ.**
 966 **submitted.** *Elegestolepis* and its kin, the earliest monodontode chondrichthyans.
 967 *Journal of Vertebrate Paleontology*.
- 968 **Bolshakova L, Ulitina L. 1985.** Stromatoporates and biostratigraphy of the Lower
 969 Paleozoic in Mongolia. *Transsec. Joint Soviet–Mongolian paleontological expedition*
 970 **27**:1–94.
- 971 **Botella H, Donoghue P, Martínez-Pérez C. 2009.** Enameloid microstructure in the
 972 oldest known chondrichthyan teeth. *Acta Zoologica* **90**:103–108.
- 973 **Brazeau MD. 2009.** The braincase and jaws of a Devonian 'acanthodian' and modern
 974 gnathostome origins. *Nature* **457**:305–308.
- 975 **Brazeau MD. 2012.** A revision of the anatomy of the Early Devonian jawed vertebrate
 976 *Ptomacanthus anglicus* Miles. *Palaeontology* **55**:355–367.
- 977 **Burrow CJ. 2003.** Redescription of the gnathostome fish fauna from the mid-
 978 Palaeozoic Silverband Formation, the Grampians, Victoria. *Alcheringa* **27**:37–49.

- 979 **Burrow CJ, Turner S. 1998.** Devonian placoderm scales from Australia. *Journal of*
980 *Vertebrate Paleontology* **18**:677–695.
- 981 **Burrow CJ, Turner S. 1999.** A review of placoderm scales, and their significance in
982 placoderm phylogeny. *Journal of Vertebrate Paleontology* **19**:204–219.
- 983 **Burrow CJ, Turner S, Wang S. 2000.** Devonian microvertebrates from Longmenshan,
984 China: Taxonomic assessment. In: Blicek A, and Turner S, eds. *Palaeozoic vertebrate*
985 *biochronology and global marine/non-marine correlation: final report of IGCP 328 (1991-*
986 *1996)*. Frankfurt a. M.: Courier Forschungsinstitut Senckenberg, 391–451.
- 987 **Davis SP, Finarelli JA, Coates MI. 2012.** *Acanthodes* and shark-like conditions in the
988 last common ancestor of modern gnathostomes. *Nature* **486**:247–250.
- 989 **Dean B. 1909.** Studies on fossil fishes (sharks, chimaeroids and arthrodires). *Memoirs*
990 *of the American Museum of Natural History* **9**:211–248.
- 991 **Denison RH. 1979.** *Acanthodii*. Stuttgart, New York: Gustav Fischer Verlag.
- 992 **Dick JR. 1981.** *Diplodoseleche woodi* gen. et sp. nov., an early Carboniferous shark
993 from the Midland Valley of Scotland. *Transactions of the Royal Society of Edinburgh:*
994 *Earth Sciences* **72**:99–113.
- 995 **Dong XIP, Donoghue PCJ, Repetski JE. 2005.** Basal tissue structure in the earliest
996 euconodonts: Testing hypotheses of developmental plasticity in euconodont phylogeny.
997 *Palaeontology* **48**:411–421.
- 998 **Donoghue PCJ. 1998.** Growth and patterning in the conodont skeleton. *Philosophical*
999 *Transactions of the Royal Society B: Biological Sciences* **353**:633–666.
- 1000 **Donoghue PCJ, Sansom IJ. 2002.** Origin and early evolution of vertebrate
1001 skeletonization. *Microscopy research and technique* **59**:352–372.

- 1002 **Donoghue PCJ, Sansom IJ, Downs JP. 2006.** Early evolution of vertebrate skeletal
- 1003 tissues and cellular interactions, and the canalization of skeletal development. *Journal*
- 1004 *of Experimental Zoology Part B: Molecular and Developmental Evolution* **306**:278–294.
- 1005 **Downs JP, and Donoghue PC. 2009.** Skeletal histology of *Bothriolepis canadensis*
- 1006 (Placodermi, Antiarchi) and evolution of the skeleton at the origin of jawed vertebrates.
- 1007 *Journal of Morphology* **270**:1364–1380.
- 1008 **Gemballa S, Bartsch P. 2002.** Architecture of the integument in lower teleostomes:
- 1009 Functional morphology and evolutionary implications. *Journal of Morphology* **253**:290–
- 1010 309.
- 1011 **Giles S, Friedman M, and Brazeau MD. 2015.** Osteichthyan-like cranial conditions in
- 1012 an Early Devonian stem gnathostome. *Nature* **520**:82–85.
- 1013 **Ginter M, Hampe O, Duffin CJ. 2010.** *Chondrichthyes: Paleozoic Elasmobranchii:*
- 1014 *Teeth*. Munich: Verlag Dr. Friedrich Pfeil.
- 1015 **Grogan ED, Lund R. 2008.** A basal elasmobranch, *Thrinacoselache gracia* n. gen and
- 1016 sp., (Thrinacodontidae, new family) from the Bear Gulch Limestone, Serpukhovian of
- 1017 Montana, USA. *Journal of Vertebrate Paleontology* **28**:970–988.
- 1018 **Grogan ED, Lund R, Greenfest-Allen E. 2012.** The origin and relationships of early
- 1019 chondrichthyans. In: Carrier JC, Musick J. A., Heithaus M. R., ed. *Biology of sharks and*
- 1020 *their relatives*. Boca Raton, FL: Taylor & Francis Inc, 3–27.
- 1021 **Gross W. 1953.** Devonische Palaeonisciden-Reste in Mittel-und Osteuropa.
- 1022 *Paläontologische Zeitschrift* **27**:85–112.
- 1023 **Gross W. 1956.** Über Crossopterygier und Dipnoer aus dem baltischen Oberdevon im
- 1024 Zusammenhang einer vergleichenden Untersuchung des Porenkanalsystems

- 1025 paläozoischer Agnathen und Fische. *Kungliga Svenska vetenskapsakademiens*
- 1026 *handlingar* **5**:1–140.
- 1027 **Gross W. 1968.** Fragliche Actinopterygier-Schuppen aus dem Silur Gotlands. *Lethaia*
- 1028 **1**:184–218.
- 1029 **Gross W. 1973.** Kleinschuppen, Flossenstacheln und Zähne von Fischen aus
- 1030 europäischen und nordamerikanischen Bonebeds des Devons. *Palaeontographica*
- 1031 *Abteilung A* **142**:51–155.
- 1032 **Hanke GF, Davis SP. 2008.** Redescription of the acanthodian *Gladiobranchus probaton*
- 1033 Bernacsek & Dineley, 1977, and comments on diplacanthid relationships. *Geodiversitas*
- 1034 **30**:303–330.
- 1035 **Hanke GF, Wilson MVH. 2004.** New teleostome fishes and acanthodian systematics.
- 1036 In: Arratia G, Wilson, M. V. H. & R. Cloutier ed. *Recent Advances in the Origin and*
- 1037 *Early Radiation of Vertebrates*. Munich: Verlag Dr. Friedrich Pfeil, 189–216.
- 1038 **Hanke GF, Wilson MVH. 2010.** The putative stem-group chondrichthyans
- 1039 *Kathemacanthus* and *Seretolepis* from the Lower Devonian MOTH locality, Mackenzie
- 1040 Mountains, Canada. In: D. K. Elliott JGM, X. Yu & D. Miao, ed. *Morphology, phylogeny*
- 1041 *and paleobiogeography of fossil fishes*. Munich: Verlag Dr. Friedrich Pfeil, 159–182.
- 1042 **Johanson Z, Smith MM, Joss JMP. 2007.** Early scale development in *Heterodontus*
- 1043 (Heterodontiformes; Chondrichthyes): a novel chondrichthyan scale pattern. *Acta*
- 1044 *Zoologica* **88**:249–256.
- 1045 **Johanson Z, Tanaka M, Chaplin N, Smith M. 2008.** Early Palaeozoic dentine and
- 1046 patterned scales in the embryonic catshark tail. *Biology letters* **4**:87–90.
- 1047 **Karatajūtė-Talimaa VN. 1973.** *Elegestolepis grossi* gen. et sp. nov., ein neuer Typ der

- 1048 Placoidschuppe aus dem Oberen Silur der Tuwa. *Palaeontographica Abt A* **143**:35–50.
- 1049 **Karatajūtė-Talimaa VN. 1992.** The early stages of the dermal skeleton formation in
- 1050 chondrichthyans. In: Mark-Kurik E, ed. *Fossil fishes as living animals*. Tallinn: Institute
- 1051 of Geology, 223–231.
- 1052 **Karatajūtė-Talimaa VN. 1995.** The Mongolepidida: scale structure and systematic
- 1053 position. *Geobios* **19**:35–37.
- 1054 **Karatajūtė-Talimaa VN. 1998.** Determination methods for the exoskeletal remains of
- 1055 early vertebrates. *Mitteilungen aus dem Museum für Naturkunde in Berlin,*
- 1056 *Geowissenschaftliche Reihe* **1**:21–51.
- 1057 **Karatajūtė-Talimaa VN, Novitskaya L. 1992.** *Teslepis*—a new representative of
- 1058 mongolepid elasmobranchs from the Lower Silurian of Mongolia. *Paleontologicheskii*
- 1059 *Zhurnal* **4**:36–46.
- 1060 **Karatajūtė-Talimaa VN, Novitskaya L. 1997.** *Sodolepis*—a new representative of
- 1061 Mongolepidida (Chondrichthyes?) from the Lower Silurian of Mongolia.
- 1062 *Paleontologicheskii Zhurnal* **5**:96–103.
- 1063 **Karatajūtė-Talimaa VN, Novitskaya L, Rozman KS, Sodov Z. 1990.** *Mongolepis*—a
- 1064 new lower Silurian genus of elasmobranchs from Mongolia. *Paleontologicheskii Zhurnal*
- 1065 **1**:76–86.
- 1066 **Karatajūtė-Talimaa VN, Smith MM. 2003.** Early acanthodians from the Lower Silurian
- 1067 of Asia. *Transactions of the Royal Society of Edinburgh: Earth Sciences* **93**:277–299.
- 1068 **Karatajūtė-Talimaa VN, Smith MM. 2004.** *Tesakoviaspis concentrica*: microskeletal
- 1069 remains of a new order of vertebrate from the Upper Ordovician and Lower Silurian of
- 1070 Siberia. In: G. Arratia MVHWR, ed. *Recent Advances in the Origin and Early Radiation*

- 1071 *of Vertebrates*. Munich, Germany: Verlag Dr. Friedrich Pfeil, 53–64.
- 1072 **Kerr T. 1952.** The scales of primitive living actinopterygians. *Proceedings of the*
- 1073 *Zoological Society of London* **122**:55–78.
- 1074 **Kerr T. 1955.** The scales of modern lungfish. *Proceedings of the Zoological Society of*
- 1075 *London* **125**:335–345.
- 1076 **Linde A. 1989.** Dentin matrix proteins: composition and possible functions in
- 1077 calcification. *The Anatomical Record* **224**:154–166.
- 1078 **Linde A, Lundgren T. 1995.** From serum to the mineral phase. The role of the
- 1079 odontoblast in calcium transport and mineral formation. *International Journal of*
- 1080 *Developmental Biology* **39**:213–213.
- 1081 **Lund R, Grogan ED. 1997.** Relationships of the Chimaeriformes and the basal
- 1082 radiation of the Chondrichthyes. *Reviews in Fish Biology and Fisheries* **7**:65–123.
- 1083 **Mader H. 1986.** *Schuppen und Zähne von Acanthodiern und Elasmobranchiern aus*
- 1084 *dem Unter-Devon Spaniens (Pisces)*. Göttingen: Geologischen Institute der Georg-
- 1085 August-Universität Göttingen.
- 1086 **Magloire H, Couble ML, Romeas A, Bleicher F. 2004.** Odontoblast primary cilia: facts
- 1087 and hypotheses. *Cell biology international* **28**:93–99.
- 1088 **Magloire H, Couble ML, Thivichon-Prince B, Maurin JC, Bleicher F. 2009.**
- 1089 Odontoblast: a mechano-sensory cell. *Journal of Experimental Zoology Part B:*
- 1090 *Molecular and Developmental Evolution* **312**:416–424.
- 1091 **Maisey J, Miller R, Turner S. 2009.** The braincase of the chondrichthyan *Doliodus* from
- 1092 the Lower Devonian Campbellton formation of New Brunswick, Canada. *Acta Zoologica*
- 1093 **90**:109–122.

- 1094 **Malzahn E. 1968.** Über neue Funde von *Janassa bituminosa* (Schloth.) im
1095 niederrheinischen Zechstein. *Geologisches Jahrbuch* **85**:67–96.
- 1096 **Märss T, Gagnier PY. 2001.** A new chondrichthyan from the Wenlock, Lower Silurian,
1097 of Baillie-Hamilton Island, the Canadian Arctic. *Journal of Vertebrate Paleontology*
1098 **21**:693–701.
- 1099 **Martínez-Pérez C, Dupret V, Manzanares E, Botella H. 2010.** New data on the Lower
1100 Devonian chondrichthyan fauna from Celtiberia (Spain). *Journal of Vertebrate*
1101 *Paleontology* **30**:1622–1627.
- 1102 **Miles RS. 1973.** Articulated acanthodian fishes from the Old Red Sandstone of
1103 England, with a review of the structure and evolution of the acanthodian shoulder-girdle.
1104 *Bulletin of the British Museum (Natural History)* **24**:111–213.
- 1105 **Miller RF, Cloutier R, Turner S. 2003.** The oldest articulated chondrichthyan from the
1106 Early Devonian period. *Nature* **425**:501–504.
- 1107 **Miyake T, Vaglia JL, Taylor LH, Hall BK. 1999.** Development of dermal denticles in
1108 skates (Chondrichthyes, Batoidea): patterning and cellular differentiation. *Journal of*
1109 *Morphology* **241**:61–81.
- 1110 **Motta P. 1977.** Anatomy and functional morphology of dermal collagen fibers in sharks.
1111 *Copeia*:454–464.
- 1112 **Murdock DJ, Dong X-P, Repetski JE, Marone F, Stampanoni M, Donoghue PC.**
1113 **2013.** The origin of conodonts and of vertebrate mineralized skeletons. *Nature* **502**:546–
1114 549.
- 1115 **Okumura R, Shima K, Muramatsu T, Nakagawa K, Shimono M, Suzuki T, Magloire**
1116 **H, Shibukawa Y. 2005.** The odontoblast as a sensory receptor cell? The expression of

- 1117 TRPV1 (VR-1) channels. *Archives of histology and cytology* **68**:251–257.
- 1118 **Ørvig T. 1966.** Histologic studies of ostracoderms, placoderms and fossil
1119 elasmobranchs. 2. On the dermal skeleton of two late Palaeozoic Elasmobranchs. *Arkiv*
1120 *för Zoologi* **19**:1–39.
- 1121 **Ørvig T. 1968.** The dermal skeleton: general considerations. In: Ørvig T, ed. *Current*
1122 *problems of lower vertebrate phylogeny*. Stockholm: Almquist and Wiksell, 374–397.
- 1123 **Ørvig T. 1977.** A survey of odontodes ('dermal teeth') from developmental, structural,
1124 functional, and phyletic points of view. In: Andrews M, R. S. & Walker, A. D., ed.
1125 *Problems in Vertebrate Evolution*. London, New York: Academic Press, 53–75.
- 1126 **Reif WE. 1978.** Types of morphogenesis of the dermal skeleton in fossil sharks.
1127 *Paläontologische Zeitschrift* **52**:110–128.
- 1128 **Reif WE. 1980.** Development of dentition and dermal skeleton in embryonic
1129 *Scyliorhinus canicula*. *Journal of Morphology* **166**:275–288.
- 1130 **Sansom IJ. 1996.** *Pseudooneotodus*: a histological study of an Ordovician to Devonian
1131 vertebrate lineage. *Zoological Journal of the Linnean Society* **118**:47–57.
- 1132 **Sansom IJ, Aldridge R, Smith M. 2000.** A microvertebrate fauna from the Llandovery
1133 of South China. *Transactions of the Royal Society of Edinburgh: Earth Sciences*
1134 **90**:255–272.
- 1135 **Sansom IJ, Davies NS, Coates MI, Nicoll RS, Ritchie A. 2012.** Chondrichthyan-like
1136 scales from the Middle Ordovician of Australia. *Palaeontology* **55**:243–247.
- 1137 **Sansom IJ, Smith MM, Smith MP. 1996.** Scales of thelodont and shark-like fishes from
1138 the Ordovician of Colorado. *Nature* **379**:628–630.
- 1139 **Sansom IJ, Smith MM, Smith MP. 2001.** The Ordovician radiation of vertebrates. In:

- 1140 Ahlberg E, ed. *Major Events in Early Vertebrate Evolution*, Systematics Association
1141 *Special Volume*. London and New York: Taylor & Francis, 156–171.
- 1142 **Sansom IJ, Wang NZ, Smith M. 2005.** The histology and affinities of sinacanthid
1143 fishes: primitive gnathostomes from the Silurian of China. *Zoological Journal of the*
1144 *Linnean Society* **144**:379–386.
- 1145 **Sasagawa I. 1995.** Evidence of two types of odontoblasts during dentinogenesis in
1146 Elasmobranchs. *Connective tissue research* **33**:223–229.
- 1147 **Schaumberg G. 1982.** *Hopleacanthus richelsdorfensis* n. g. n. sp., ein Euselachier aus
1148 dem permischen Kupferschiefer von Hessen (W-Deutschland). *Paläontologische*
1149 *Zeitschrift* **56**:235–257.
- 1150 **Schmidt WJ, Keil A. 1971.** *Polarizing microscopy of dental tissues*: Pergamon Press.
- 1151 **Schultze H-P. 1968.** Palaeoniscoidea-Schuppen aus dem Unterdevon Australiens und
1152 Kanadas und aus dem Mitteldevon Spitzbergens. *Bulletin of the British Museum*
1153 *(Natural History)* **16**:343–368.
- 1154 **Sennikov N, Rodina O, Izokh N, Obut O. 2015.** New data on Silurian vertebrates of
1155 southern Siberia. *Palaeoworld* **24**:231–242.
- 1156 **Servais T, Owen AW, Harper DA, Kröger B, Munnecke A. 2010.** The great ordovician
1157 biodiversification event (GOBE): the palaeoecological dimension. *Palaeogeography,*
1158 *Palaeoclimatology, Palaeoecology* **294**:99–119.
- 1159 **Sire JY. 1994.** Light and TEM study of nonregenerated and experimentally regenerated
1160 scales of *Lepisosteus oculatus* (Holostei) with particular attention to ganoine formation.
1161 *The Anatomical Record* **240**:189–207.
- 1162 **Sire JY. 2005.** Development and fine structure of the bony scutes in *Corydoras*

1163 *arcuatus* (Siluriformes, Callichthyidae). *Journal of Morphology* **215**:225–244.

1164 **Sire JY, Donoghue PCJ, Vickaryous MK. 2009.** Origin and evolution of the
 1165 integumentary skeleton in non-tetrapod vertebrates. *Journal of anatomy* **214**:409–440.

1166 **Sire JY, Huysseune A. 1996.** Structure and development of the odontodes in an
 1167 armoured catfish, *Corydoras aeneus* (Siluriformes, Callichthyidae). *Acta Zoologica*
 1168 **77**:51–72.

1169 **Sire JY, Huysseune A. 2003.** Formation of dermal skeletal and dental tissues in fish: a
 1170 comparative and evolutionary approach. *Biological Reviews* **78**:219–249.

1171 **Smith MM. 1979.** Scanning electron microscopy of odontodes in the scales of a
 1172 coelacanth embryo, *Latimeria chalumnae* Smith. *Archives of oral biology* **24**:179–183.

1173 **Smith MM, Hall BK. 1993.** A developmental model for evolution of the vertebrate
 1174 exoskeleton and teeth. *Evolutionary biology*: Springer, 387–448.

1175 **Smith MM, Hobdell MH, Miller W. 1972.** The structure of the scales of *Latimeria*
 1176 *chalumnae*. *Journal of Zoology* **167**:501–509.

1177 **Smith MM, Sansom IJ, Smith MP. 1996.** 'Teeth' before armour: The earliest vertebrate
 1178 mineralized tissues. *Modern Geology* **20**:303–319.

1179 **Stahl BJ. 1999.** *Chondrichthyes III: Holocephali*. Munich: Verlag Dr. Friedrich Pfeil.

1180 **Thorsteinsson R. 1973.** Dermal elements of a new lower vertebrate from Middle
 1181 Silurian (Upper Wenlockian) Rocks of the Canadian Arctic Archipelago.
 1182 *Palaeontographica Abteilung A* **143**:51–57.

1183 **Turner S, Blieck A, Nowlan G. 2004.** Vertebrates (agnathans and gnathostomes). In:
 1184 Webby BD, Paris F, Droser ML, and Percival I, eds. *The Great Ordovician*
 1185 *Biodiversification Event*: Columbia University Press, 327–335.

- 1186 **Valiukevičius J. 1992.** First articulated *Poracanthodes* from the Lower Devonian of
- 1187 Severnaya Zemlya. In: Mark-Kurik E, ed. *Fossil Fishes as Living Animals*. Tallinn:
- 1188 Academy of Sciences of Estonia, 193–214.
- 1189 **Valiukevičius J. 2003.** Devonian acanthodians from Severnaya Zemlya Archipelago
- 1190 (Russia). *Geodiversitas* **25**:131–204.
- 1191 **Valiukevičius J, Burrow CJ. 2005.** Diversity of tissues in acanthodians with
- 1192 *Nostolepis*-type histological structure. *Acta Palaeontologica Polonica* **50**:635–649.
- 1193 **Wang N-Z, Zhang S-B, Wang J-Q, Zhu M. 1998.** Early Silurian chondrichthyan
- 1194 microfossils from Bachu County, Xinjiang, China. *Vertebrata Palasiatica* **36**:257–267.
- 1195 **Wang R. 1993.** *Taxonomie, Palökologie und Biostratigraphie der Mikroichthyolithen aus*
- 1196 *dem Unterdevon Keltiberiens, Spanien*. Frankfurt a. M.: Senckenbergische
- 1197 Naturforschende Gesellschaft.
- 1198 **Webby BD, Paris F, Droser ML. 2004.** *The great Ordovician biodiversification event*.
- 1199 New York: Columbia University Press.
- 1200 **Williams ME. 1998.** A new specimen of *Tamiobatis vetustus* (Chondrichthyes,
- 1201 Ctenacanthoidea) from the late Devonian Cleveland Shale of Ohio. *Journal of*
- 1202 *Vertebrate Paleontology* **18**:251–260.
- 1203 **Yoshida K, Yoshida N, Ejiri S, Iwaku M, Ozawa H. 2002.** Odontoblast processes in
- 1204 human dentin revealed by fluorescence labeling and transmission electron microscopy.
- 1205 *Histochemistry and cell biology* **118**:205–212.
- 1206 **Young G. 1982.** Devonian sharks from south-eastern Australia and Antarctica.
- 1207 *Palaeontology* **25**:817–843.
- 1208 **Zangerl R. 1966.** A new shark of the family Edestidae, *Ornithoprion hertwigi*, from the

- 1209 Pennsylvanian Mecca and Logan quarry shales of Indiana. *Fieldiana: Geology* **16**:1–43.
- 1210 **Zangerl R. 1968.** The morphology and the developmental history of the scales of the
- 1211 Paleozoic sharks *Holmesella?* sp. and *Orodus*. In: Ørvig T, ed. *Current Problems of*
- 1212 *Lower Vertebrate Phylogeny*. Stockholm: Almqvist & Wiksell, 399–412.
- 1213 **Zangerl R. 1981.** *Chondrichthyes I: Paleozoic Elasmobranchii*. Stuttgart and New York:
- 1214 Gustav Fischer.
- 1215 **Zeng XY. 1988.** Some fin-spines of Acanthodii from Early Silurian of Hunan, China.
- 1216 *Vertebrata Palasiatica* **26**:287-295.
- 1217 **Zhu M. 1998.** Early Silurian sinacanth (Chondrichthyes) from China. *Palaeontology*
- 1218 **41**:157–172.
- 1219 **Zhu M, Yu X, Ahlberg PE, Choo B, Lu J, Qiao T, Qu Q, Zhao W, Jia L, Blom H.**
- 1220 **2013.** A Silurian placoderm with osteichthyan-like marginal jaw bones. *Nature* **502**:188–
- 1221 193.
- 1222 **Žigaitė Ž, Karatajūtė-Talimaa V, Blieck A. 2011.** Vertebrate microremains from the
- 1223 Lower Silurian of Siberia and Central Asia: palaeobiodiversity and palaeobiogeography.
- 1224 *Journal of Micropalaeontology* **30**:97–106.
- 1225
- 1226
- 1227
- 1228
- 1229

1230

1231

1232

1233

1234

1235

1236

1237

1238

1239

1240 **Figure captions**

1241 **Figure 1 Principle morphological features of scales.** Line drawing of a *Mongolepis*
1242 scale (BU5296) from the Chargat Formation of north-western Mongolia in lateral view.

1243 **Figure 2 Scale morphology of Mongolepididae.** (A–C) *Mongolepis rozmanae* scale
1244 BU5296 (Chargat Formation, north-western Mongolia) in (A) anterior (B) lateral, (C) and
1245 basal aspect and a *M. rozmanae* scale in (D) crown view (BU5351, Chargat Formation,

1246 north-western Mongolia); (E, G) *Teslepis jucunda* BU5322 (Chargat Formation, north-
 1247 western Mongolia) in (E) crown and (G) basal view and a *T. jucunda* scale (BU5352,
 1248 Chargat Formation, north-western Mongolia) in an (F) antero-lateral view; (H–J)
 1249 *Sodolepis lucens* scales (Chargat Formation, north-western Mongolia) in (H) lateral
 1250 (BU5305), crown (BU5304) and (J) basal (BU5355) views; (K–M) *Rongolepis cosmetica*
 1251 scale BU5303 (Xiushan Formation, south China) in (K) crown, (L) lateral and (M) basal
 1252 views;. Volume renderings, (A–C), (H) and (K–M); SEM micrographs, (D–G) and (I, J).
 1253 Crown and base foramina indicated by arrows and arrowheads respectively. Anterior to
 1254 the left in (B), (H), (L) and bottom in (A–G), (H–K), (M). Scale bar equals 500 μm in (D,
 1255 I, J), 400 μm in (A–C), 300 μm in (H, K) and 200 μm in (E–G, L, M).

1256 Figure 3 **Scale morphology of Shiqianolepidae.** (A–C) *Shiqianolepis hollandi* scales
 1257 (Xiushan Formation, south China) in (A) lateral (NIGP 130307), (B) crown (NIGP
 1258 130309) and (C) postero-basal (NIGP 130307) views; (D–F) *Xinjiangichthys*
 1259 *pluridentatus* scale IVPP V X2 (Yimugantawu Formation, north-western China) in (D)
 1260 anterior, (E) posterior and (F) antero-lateral views. All images volume renderings except
 1261 (B). Crown foramina indicated by arrows. Anterior to the left in (A), to the right in (F) and
 1262 bottom in (B). Scale bar equals 300 μm in (A, B) and 200 μm in (C–F).

1263 Figure 4 **SEM micrographs of *Solinalepis levis* gen. et sp. nov. scales from the**
 1264 **Upper Ordovician Harding Sandstone of Colorado, USA.** (A–C) tessera-like head
 1265 scales in (A, B) crown (BU5307, BU5308) and (C) lateral (BU5309) views; (D) bulbous
 1266 head scale (BU5312) in lateral view; (E–I) polygonal trunk scales, (E) holotype
 1267 (BU5310) in anterior view, (F) BU5345 in crown, (G) corono-lateral and (H) partial
 1268 posterior views, (I) BU5313 in basal view; J–L, lanceolate trunk scales in (J) anterior

1269 (BU5314), (K) lateral (BU5315) and (L) posterior (BU5311) views. Base foramina
1270 indicated by arrowheads. Anterior to the left in (G) and (K). Scale bar equals 300 μ m
1271 in (A, B), 200 μ m in (C), 100 μ m in (D–G, I–L), and 50 μ m in (H).

1272 **Figure 5 Scale histology of Mongolian and Chinese mongolepids.** (A) medial
1273 longitudinal section of a *Mongolepis rozmanae* scale (BU5297; Chargat Formation,
1274 north-western Mongolia); (B) detail of (A) depicting primary and secondary odontodes at
1275 the anterior crown margin; (C) primary odontode lamellin microstructure in a
1276 longitudinally sectioned *Mongolepis rozmanae* scale (BU5298; Chargat Formation,
1277 north-western Mongolia), etched for 10 min in 0.5% orthophosphoric acid; (D) basal
1278 bone microstructure of a longitudinally sectioned *Mongolepis rozmanae* scale (BU5354;
1279 Chargat Formation, north-western Mongolia) etched for 10 min in 0.5% orthophosphoric
1280 acid; (E) detail of BU5354 depicting the bone tissue of the anterior basal platform; (F)
1281 medial longitudinal section of a *Teslepis jucunda* scale (BU5324; Chargat Formation,
1282 north-western Mongolia); (G) lamellin architecture of two odontodes in a longitudinally
1283 sectioned *Sodolepis lucens* scale (BU5306; Chargat Formation, north-western
1284 Mongolia) etched for 10 min in 0.5% orthophosphoric acid; (H) basal bone
1285 microstructure in BU5306 at the anterior projection of the base; (I), sagittal longitudinal
1286 section of a *Sodolepis lucens* scale (BU5344; Chargat Formation, north-western
1287 Mongolia); (J) anterior third of BU5306 showing the contact between the globular crown
1288 dentine and the underlying basal bone; (K) sagittal longitudinal section of a *Rongolepis*
1289 *cosmetica* scale (NIGP 130328; Xiushan Formation, south China); (L) detail of NIGP
1290 130328 showing the mid third of the scale crown; (M) *Xinjiangichthys pluridentatus*
1291 scale (IVPP V X1; Yimugantawu Formation, north-western China) in longitudinal

section; (N) sagittal longitudinal section of a *Shiqianolepis hollandi* trunk scale (NIGP 130312; Xiushan Formation, south China). Nomarski differential interference contrast optics micrographs, (A), (B), (D), (F), (G), (I) and (K–N); SEM micrographs, (C), (E), (H) and (J). Anterior towards the left in (A–J, L) and towards the right in (K), (M) and (N). Abbreviations: gb, globular dentine; lb, lamellar bone; red dotted lines, contact surfaces between primary and secondary odontodes; white dotted lines, border between globular dentine and basal bone; white dashed line, contact surfaces between primary odontodes in *Rongolepis*. Asterisks mark bone layers with fibre orientation parallel to the section axis. Scale bar equals 400 μm in (A), 100 μm in (B, G, H, M), 20 μm in (C), 200 μm in (D, F, K, N), 50 μm in (E, J, L), and 300 μm in (I).

Figure 6 Histology of *Solinalepis levis* gen. et sp. nov. scales. (A) thin-sectioned head scale (BU5317) from the Harding Sandstone, Colorado, USA; (B) transverse section of a *Solinalepis levis* gen. et sp. nov. trunk scale (BU5316) from the Harding Sandstone, Colorado, USA. Scale bar equals 200 μm in (A) and 100 μm in (B).

Figure 7 Canal system of mongolepid scales. Volume renderings. (A–C) canals (red) inside a translucent *Mongolepis rozmanae* scale (BU5296) in (A) lateral view, in (B) posterior view sliced along the plane 1 and in (C, C1) crown view sliced along plane 2; (D, D1) canals in a transversely sliced *Teslepis jucunda* scale (BU5325) shown in posterior view; (E) pulp cavities (red) in a transversely sliced *Sodolepis lucens* scale (BU5305) shown in postero-lateral view; (F) longitudinally sliced *Shiqianolepis hollandi* scale (NIGP 130307) in baso-lateral view; (G, H) longitudinally sliced *Xinjiangichthys pluridentatus* scale IVPP V X2 in (G) posterior and (H) lateral views; (I, J) canals system (red) inside a transversely sliced *Solinalepis levis* gen. et sp. nov. scale (BU5318)

1315 shown in posterior view, (J) detail of (I). Horizontal canals depicted in purple in c1 and
 1316 d1. Yellow arrowheads point at canal openings on the sub-crown surface. Red dotted
 1317 line, contact surfaces between primary and secondary odontodes; grey dotted line,
 1318 crown/base border. Scale bar equals 400 μm in (A–C), 100 μm in (D, H, I), 200 μm in
 1319 (E), 300 μm (F, G) and 50 μm in (J).

1320 **Figure 8 Odontocomplex organization of mongolepid scale crowns.** (A) *Teslepis*
 1321 *jucunda* (BU5323) scale, medial portion of the crown; (B) *Shiqianolepis hollandi* (NIGP
 1322 130309) scale, medial portion of the crown; (C) *Solinalepis levis* gen. et sp. nov. trunk
 1323 scale (BU5314), lateral portion of the crown. Primary odontocomplex structure in
 1324 Mongolepidida demonstrated by line drawings of longitudinally sectioned (D)
 1325 *Mongolepis rozmanae* (BU5297) and (E) *Shiqianolepis hollandi* (NIGP 130312) scales.
 1326 In (A–C) some of the odontocomplexes are highlighted in red and green. Dark green
 1327 and dark red, odd numbered odontodes; light green and light red, even numbered
 1328 odontodes. In (D, E)—light grey, primary odontodes; light yellow, secondary odontodes.
 1329 Anterior towards the bottom in (A–C) and towards the left in (D, E). Scale bar equals
 1330 100 μm in (A), 200 μm in (B) and 50 μm in (C).

1331

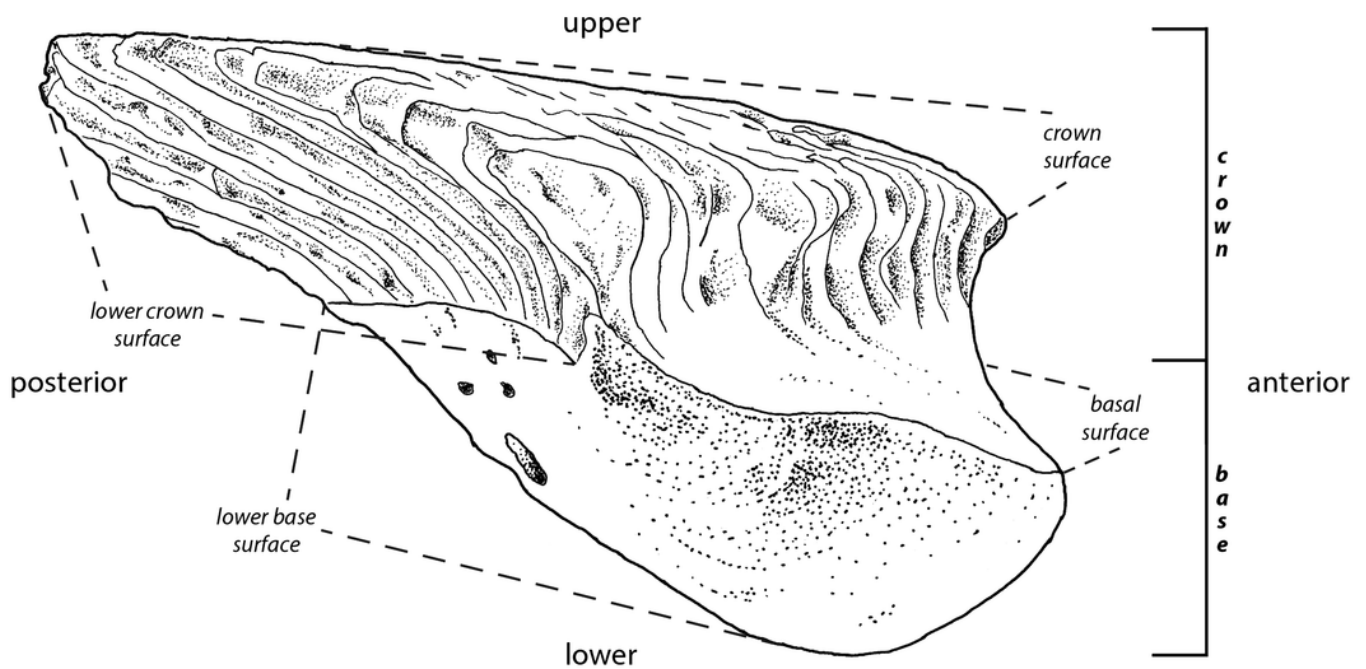
1332

1333

1

Principle morphological features of scales

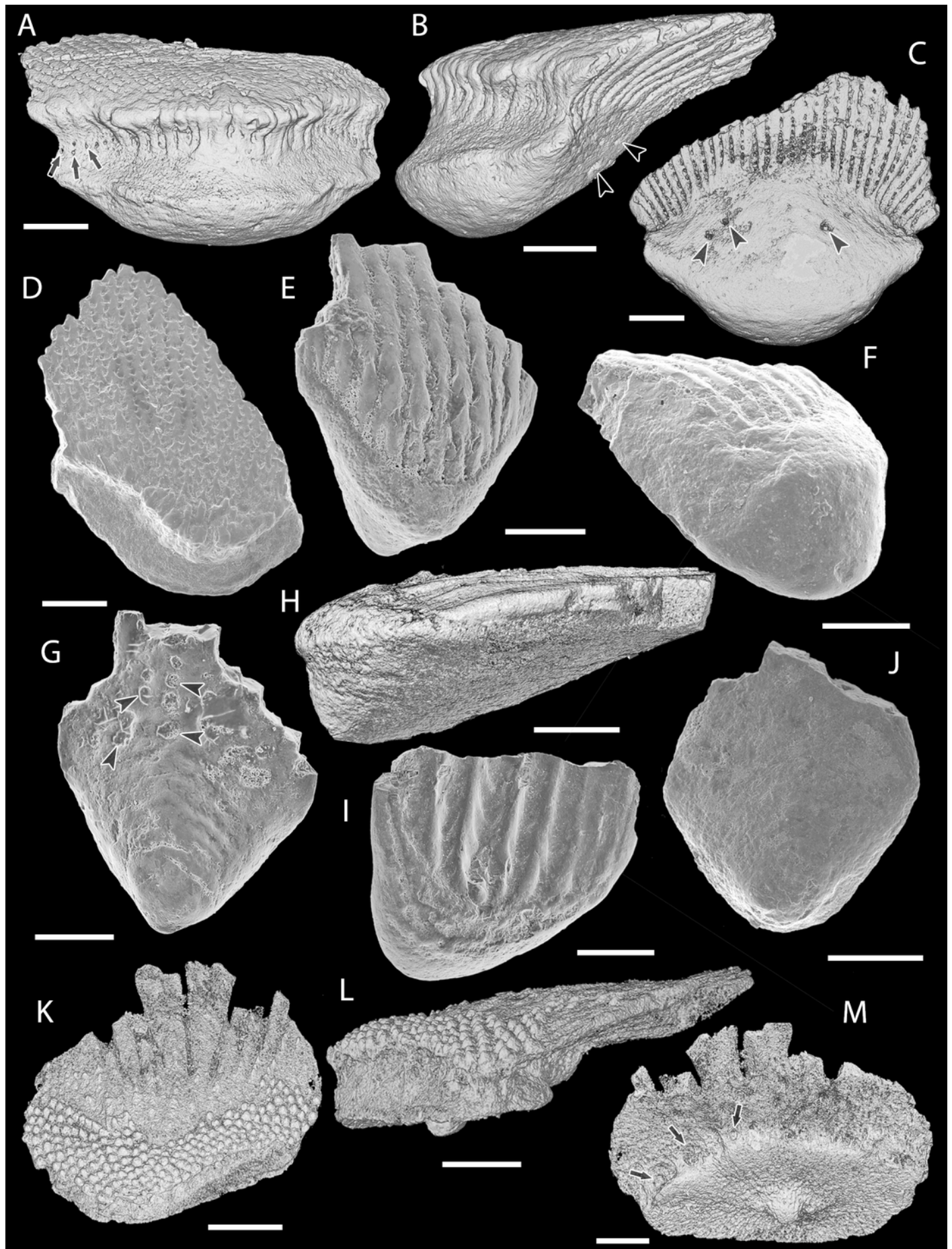
Figure 1 **Principle morphological features of scales.** Line drawing of a *Mongolepis* scale (BU5296) from the Chargat Formation of north-western Mongolia in lateral view.



2

Scale morphology of Mongolepididae

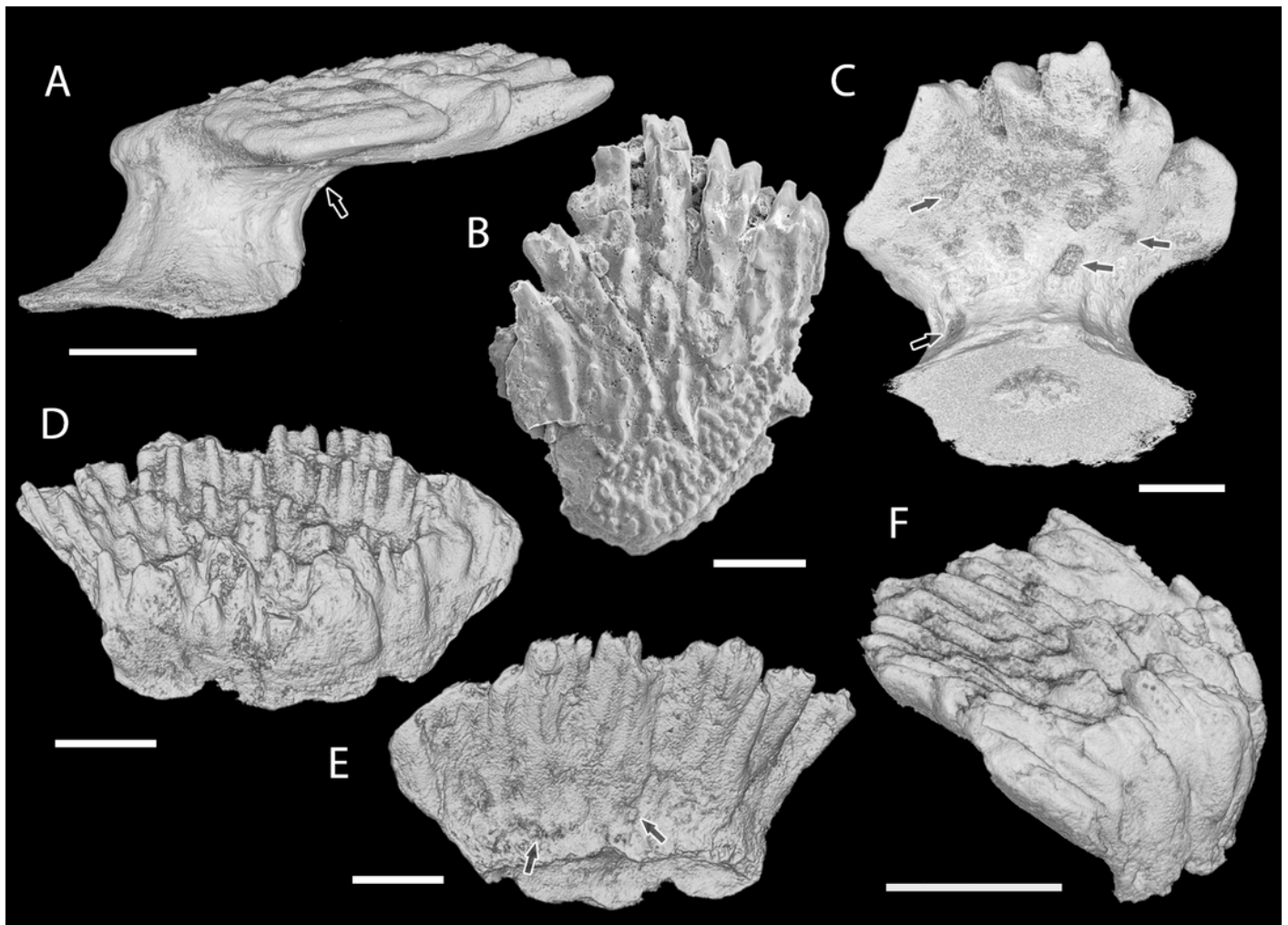
Figure 2 **Scale morphology of Mongolepididae.** (A–C) *Mongolepis rozmanae* scale BU5296 (Chargat Formation, north-western Mongolia) in (A) anterior (B) lateral, (C) and basal aspect and a *M. rozmanae* scale in (D) crown view (BU5351, Chargat Formation, north-western Mongolia); (E, G) *Teslepis jucunda* BU5322 (Chargat Formation, north-western Mongolia) in (E) crown and (G) basal view and a *T. jucunda* scale (BU5352, Chargat Formation, north-western Mongolia) in an (F) antero-lateral view; (H–J) *Sodolepis lucens* scales (Chargat Formation, north-western Mongolia) in (H) lateral (BU5305), crown (BU5304) and (J) basal (BU5355) views; (K–M) *Rongolepis cosmetica* scale BU5303 (Xiushan Formation, south China) in (K) crown, (L) lateral and (M) basal views;. Volume renderings, (A–C), (H) and (K–M); SEM micrographs, (D–G) and (I, J). Crown and base foramina indicated by arrows and arrowheads respectively. Anterior to the left in (B), (H), (L) and bottom in (A–G), (H–K), (M). Scale bar equals 500 μm in (D, I, J), 400 μm in (A–C), 300 μm in (H, K) and 200 μm in (E–G, L, M).



3

Scale morphology of Shiqianolepidae

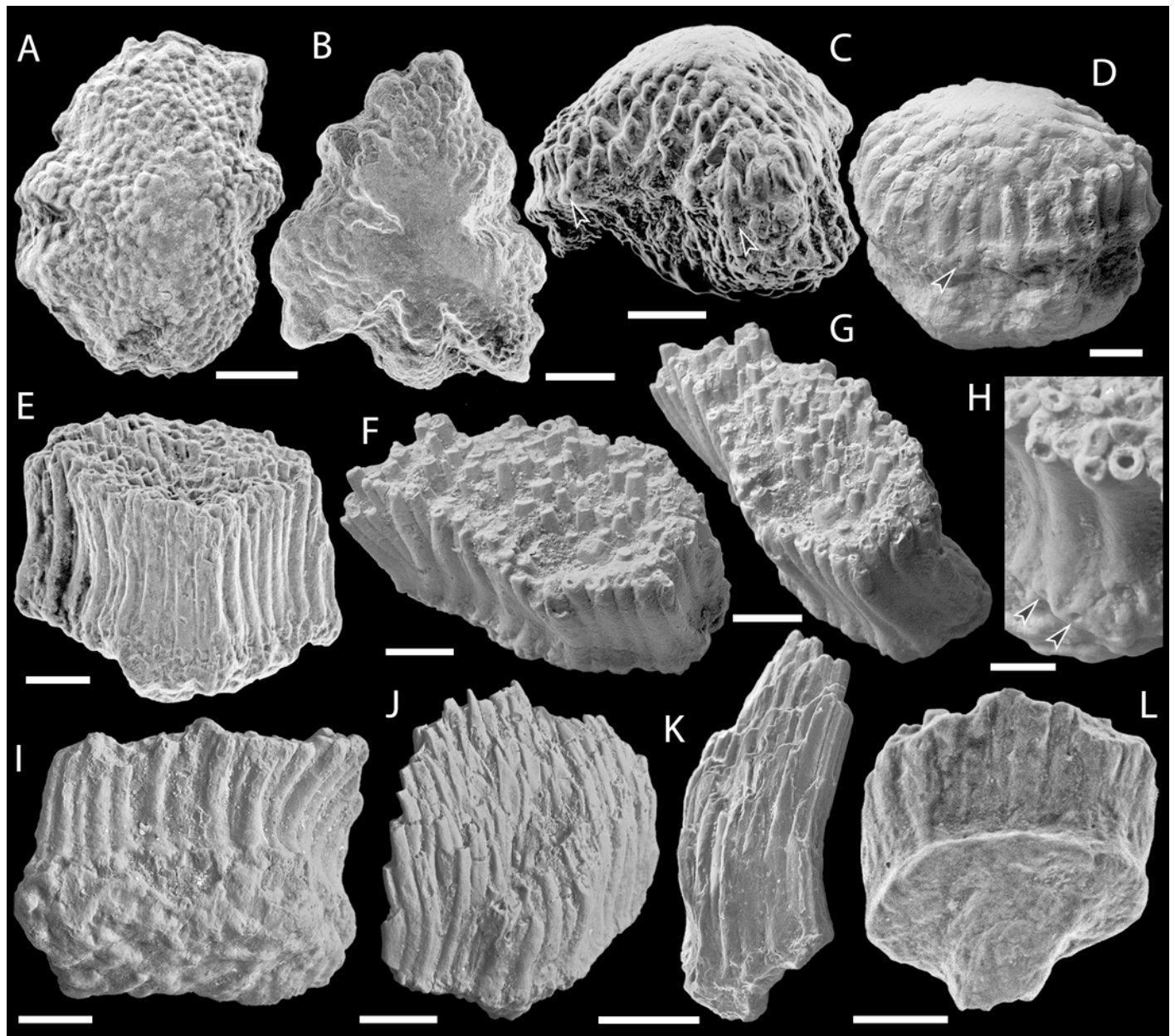
Figure 3 **Scale morphology of Shiqianolepidae.** (A-C) *Shiqianolepis hollandi* scales (Xiushan Formation, south China) in (A) lateral (NIGP 130307), (B) crown (NIGP 130309) and (C) postero-basal (NIGP 130307) views; (D-F) *Xinjiangichthys pluridentatus* scale IVPP V X2 (Yimugantawu Formation, north-western China) in (D) anterior, (E) posterior and (F) antero-lateral views. All images volume renderings except (B). Crown foramina indicated by arrows. Anterior to the left in (A), to the right in (F) and bottom in (B). Scale bar equals 300 μm in (A, B) and 200 μm in (C-F).



4

Solinalepis levis gen. et sp. nov. scales

Figure 4 **SEM micrographs of *Solinalepis levis* gen. et sp. nov. scales from the Upper Ordovician Harding Sandstone of Colorado, USA.** (A–C) tessera-like head scales in (A, B) crown (BU5307, BU5308) and (C) lateral (BU5309) views; (D) bulbous head scale (BU5312) in lateral view; (E–I) polygonal trunk scales, (E) holotype (BU5310) in anterior view, (F) BU5345 in crown, (G) corono-lateral and (H) partial posterior views, (I) BU5313 in basal view; J–L, lanceolate trunk scales in (J) anterior (BU5314), (K) lateral (BU5315) and (L) posterior (BU5311) views. Base foramina indicated by arrowheads. Anterior to the left in (G) and (K). Scale bar equals 300 μm in (A, B), 200 μm in (C), 100 μm in (D–G, I–L), and 50 μm in (H).

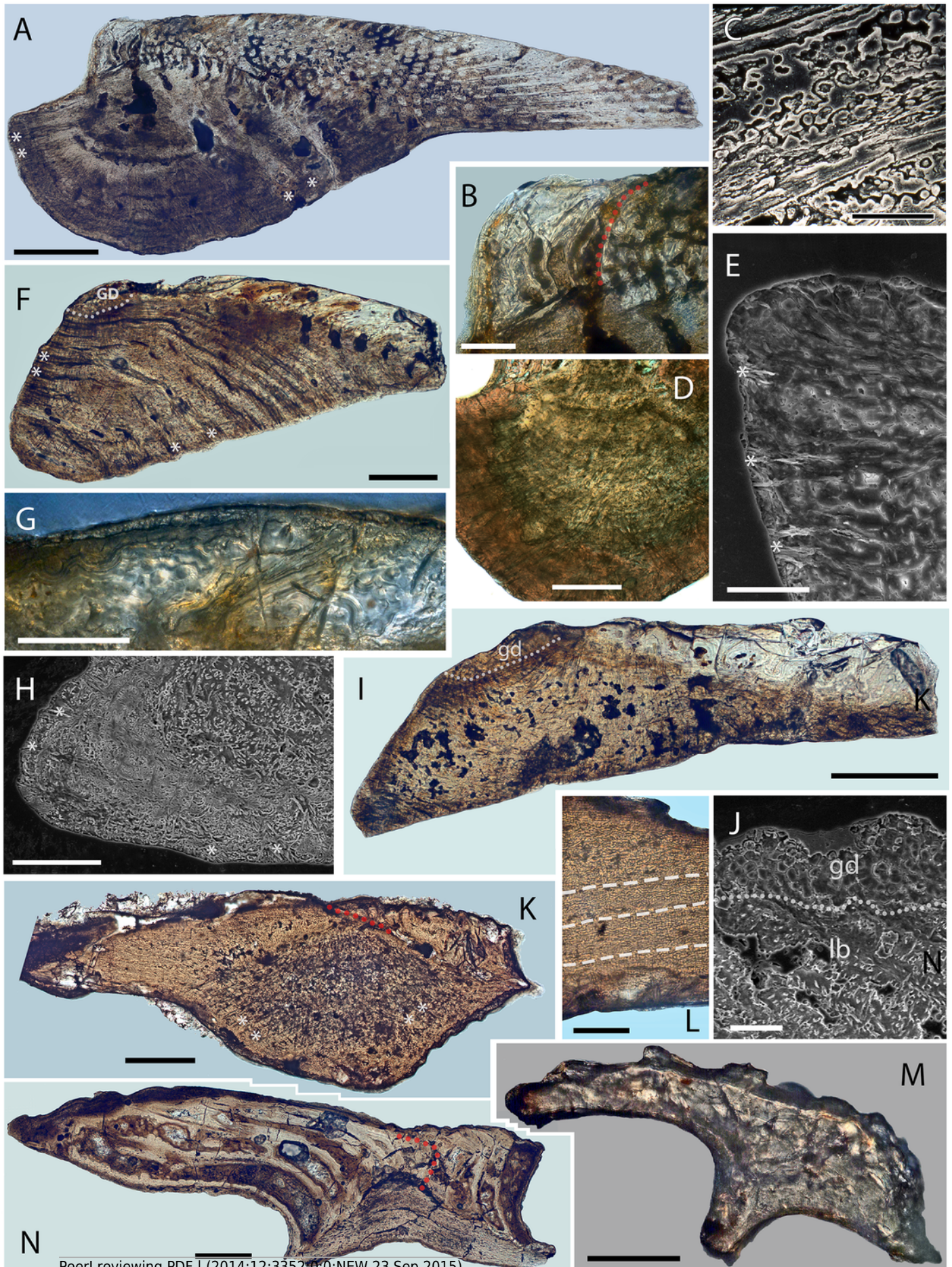


5

Scale histology of Mongolian and Chinese mongolepids

Figure 5 **Scale histology of Mongolian and Chinese mongolepids.** (A) medial longitudinal section of a *Mongolepis rozmanae* scale (BU5297; Chagat Formation, north-western Mongolia); (B) detail of (A) depicting primary and secondary odontodes at the anterior crown margin; (C) primary odontode lamellin microstructure in a longitudinally sectioned *Mongolepis rozmanae* scale (BU5298; Chagat Formation, north-western Mongolia), etched for 10 min in 0.5% orthophosphoric acid; (D) basal bone microstructure of a longitudinally sectioned *Mongolepis rozmanae* scale (BU5354; Chagat Formation, north-western Mongolia) etched for 10 min in 0.5% orthophosphoric acid; (E) detail of BU5354 depicting the bone tissue of the anterior basal platform; (F) medial longitudinal section of a *Teslepis jucunda* scale (BU5324; Chagat Formation, north-western Mongolia); (G) lamellin architecture of two odontodes in a longitudinally sectioned *Sodolepis lucens* scale (BU5306; Chagat Formation, north-western Mongolia) etched for 10 min in 0.5% orthophosphoric acid; (H) basal bone microstructure in BU5306 at the anterior projection of the base; (I), sagittal longitudinal section of a *Sodolepis lucens* scale (BU5344; Chagat Formation, north-western Mongolia); (J) anterior third of BU5306 showing the contact between the globular crown dentine and the underlying basal bone; (K) sagittal longitudinal section of a *Rongolepis cosmetica* scale (NIGP 130328; Xiushan Formation, south China); (L) detail of NIGP 130328 showing the mid third of the scale crown; (M) *Xinjiangichthys pluridentatus* scale (IVPP V X1; Yimugantawu Formation, north-western China) in longitudinal section; (N) sagittal longitudinal section of a *Shiqianolepis hollandi* trunk scale (NIGP 130312; Xiushan Formation, south China). Nomarski differential interference contrast optics micrographs, (A), (B), (D), (F), (G), (I) and (K–N); SEM micrographs, (C), (E), (H) and (J). Anterior towards the left in (A–J, L) and towards the right in (K), (M) and (N). Abbreviations: gb, globular dentine; lb, lamellar bone; red dotted lines, contact surfaces between primary and secondary odontodes; white

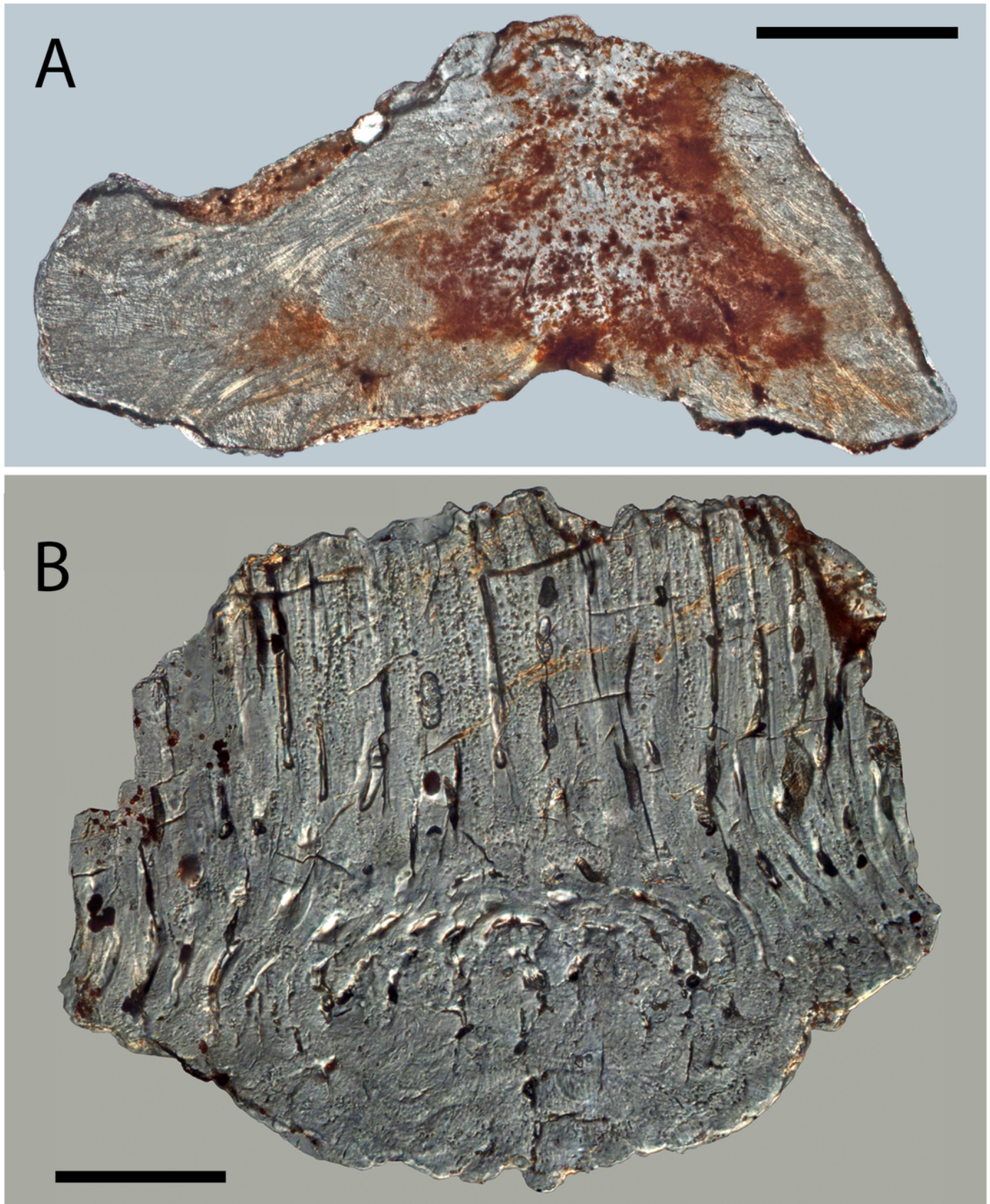
dotted lines, border between globular dentine and basal bone; white dashed line, contact surfaces between primary odontodes in *Rongolepis*. Asterisks mark bone layers with fibre orientation parallel to the section axis. Scale bar equals 400 μm in (A), 100 μm in (B, G, H, M), 20 μm in (C), 200 μm in (D, F, K, N), 50 μm in (E, J, L), and 300 μm in (I).



6

Histology of *Solinalepis levis* gen. et sp. nov. scales

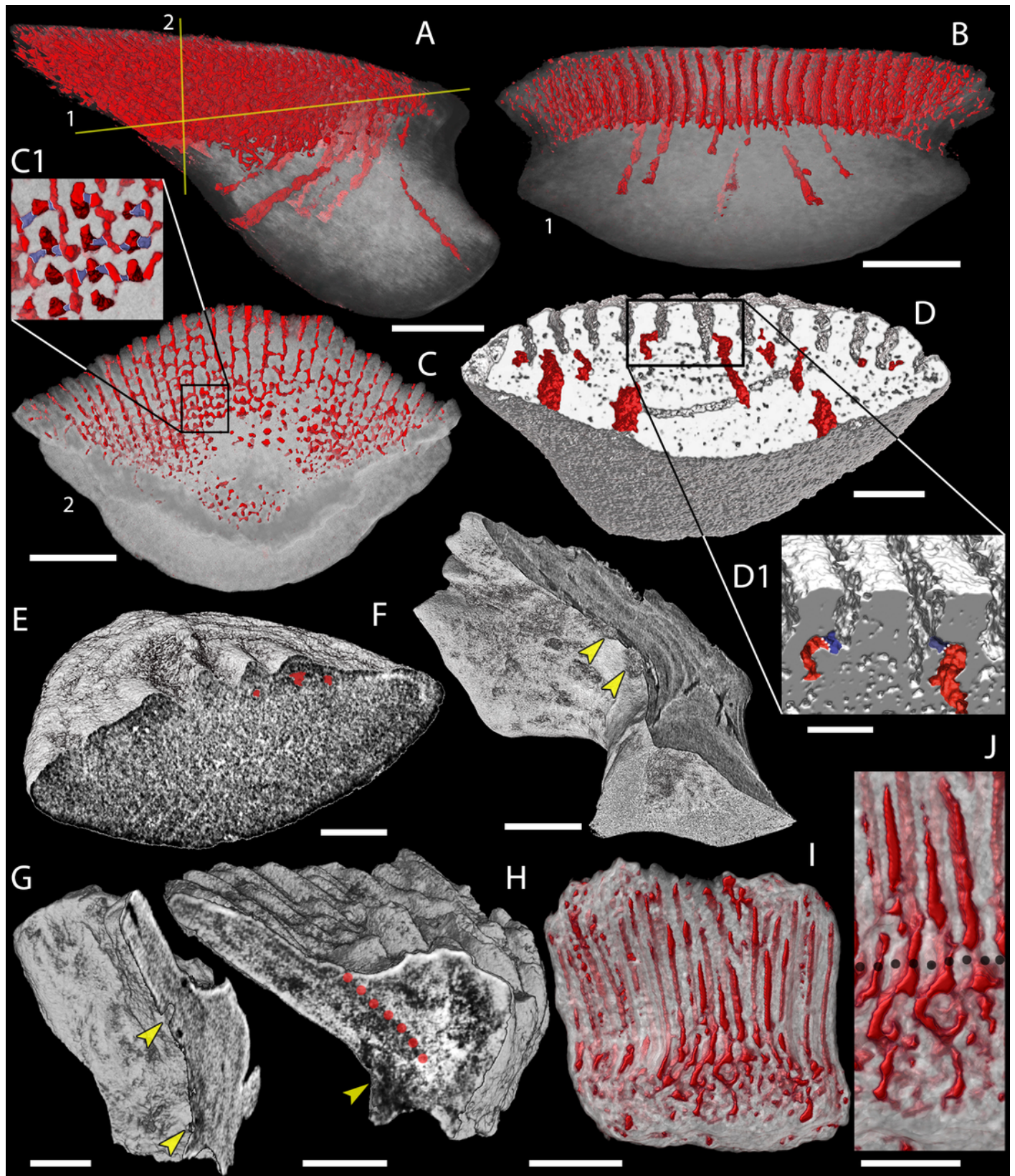
Figure 6 **Histology of *Solinalepis levis* gen. et sp. nov. scales.** (A) thin-sectioned head scale (BU5317) from the Harding Sandstone, Colorado, USA; (B) transverse section of a *Solinalepis levis* gen. et sp. nov. trunk scale (BU5316) from the Harding Sandstone, Colorado, USA. Scale bar equals 200 μm in (A) and 100 μm in (B).



7

Canal system of mongolepid scales

Figure 7 **Canal system of mongolepid scales.** Volume renderings. (A–C) canals (red) inside a translucent *Mongolepis rozmanae* scale (BU5296) in (A) lateral view, in (B) posterior view sliced along the plane 1 and in (C, C1) crown view sliced along plane 2; (D, D1) canals in a transversely sliced *Teslepis jucunda* scale (BU5325) shown in posterior view; (E) pulp cavities (red) in a transversely sliced *Sodolepis lucens* scale (BU5305) shown in postero-lateral view; (F) longitudinally sliced *Shiqianolepis hollandi* scale (NIGP 130307) in baso-lateral view; (G, H) longitudinally sliced *Xinjiangichthys pluridentatus* scale IVPP V X2 in (G) posterior and (H) lateral views; (I, J) canals system (red) inside a transversely sliced *Solinalepis levis* gen. et sp. nov. scale (BU5318) shown in posterior view, (J) detail of (I). Horizontal canals depicted in purple in c1 and d1. Yellow arrowheads point at canal openings on the sub-crown surface. Red dotted line, contact surfaces between primary and secondary odontodes; grey dotted line, crown/base border. Scale bar equals 400 μm in (A–C), 100 μm in (D, H, I), 200 μm in (E), 300 μm (F, G) and 50 μm in (J).



8

Odontocomplex organization of mongolepid scale crowns

Figure 8 **Odontocomplex organization of mongolepid scale crowns.** (A) *Teslepis jucunda* (BU5323) scale, medial portion of the crown; (B) *Shiqianolepis hollandi* (NIGP 130309) scale, medial portion of the crown; (C) *Solinalepis levis* gen. et sp. nov. trunk scale (BU5314), lateral portion of the crown. Primary odontocomplex structure in Mongolepidida demonstrated by line drawings of longitudinally sectioned (D) *Mongolepis rozmanae* (BU5297) and (E) *Shiqianolepis hollandi* (NIGP 130312) scales. In (A-C) some of the odontocomplexes are highlighted in red and green. Dark green and dark red, odd numbered odontodes; light green and light red, even numbered odontodes. In (D, E)—light grey, primary odontodes; light yellow, secondary odontodes. Anterior towards the bottom in (A-C) and towards the left in (D, E). Scale bar equals 100 μm in (A), 200 μm in (B) and 50 μm in (C).

